AD_____

Award Number: W81XWH-06-1-0059

TITLE: Cell cycle dependence of TRIAL sensitivity in prostate cancer cells

PRINCIPAL INVESTIGATOR: David J. McConkey, Ph.D.

CONTRACTING ORGANIZATION: University of Texas
M.D. Anderson Cancer Center
Houston, TX 77030

REPORT DATE: November 2007

TYPE OF REPORT: Annual

PREPARED FOR: U.S. Army Medical Research and Materiel Command
Fort Detrick, Maryland 21702-5012

REPORT DOCUMENTATION PAGE

Form Approved
OMB No. 0704-0188

1. REPORT DATE	2. REPORT TYPE	3. DATES COVERED
23-11-2007	Annual	24 OCT 2006 - 23 OCT 2007

4. TITLE AND SUBTITLE
Cell cycle dependence of TRIAL sensitivity in prostate cancer cells

5a. CONTRACT NUMBER

5b. GRANT NUMBER
W81XWH-06-1-0059

5c. PROGRAM ELEMENT NUMBER

6. AUTHOR(S)
David J. McConkey, Ph.D.

Email: dmcconke@notes.mdacc.tmc.edu

5d. PROJECT NUMBER

5e. TASK NUMBER

5f. WORK UNIT NUMBER

7. PERFORMING ORGANIZATION NAME(S) AND ADDRESS(ES)

University of Texas
M.D. Anderson Cancer Center
Houston, TX 77030

8. PERFORMING ORGANIZATION REPORT NUMBER

9. SPONSORING / MONITORING AGENCY NAME(S) AND ADDRESS(ES)
U.S. Army Medical Research and Materiel Command
Fort Detrick, Maryland 21702-5012

10. SPONSOR/MONITOR'S ACRONYM(S)

11. SPONSOR/MONITOR'S REPORT NUMBER(S)

12. DISTRIBUTION / AVAILABILITY STATEMENT
Approved for Public Release; Distribution Unlimited

13. SUPPLEMENTARY NOTES

14. ABSTRACT

The proteasome inhibitor bortezomib (PS-341, Velcade) synergizes with tumor necrosis factor-related apoptosis-inducing ligand (TRAIL) acts via a p21-dependent mechanism to induce high levels of apoptosis in prostate cancer cells. Our further investigation into the molecular mechanisms underlying the effects of bortezomib implicated endoplasmic reticular (ER) stress in its anti-tumoral effects. These effects also provide us with a molecular mechanism to explain the observed anti-angiogenic effects of bortezomib in prostate cancer cells. We have generated luciferase-transduced variants of our human prostate cancer cell lines in order to use them to generate orthotopic tumors in nude mice that can be imaged non-invasively. We plan to use these models in the coming 6-12 months to test the toxicity and anti-tumoral efficacy of combination therapy with bortezomib plus anti-DR5 antibodies in vivo. Preliminary toxicity studies confirmed that mice tolerate daily therapy with recombinant TRAIL plus biweekly therapy with bortezomib (at its MTD) very well.

15. SUBJECT TERMS

PROTEASOME INHIBITOR, P21, CYCLIN-DEPENDENT KINASE, XENOGRAFTS

16. SECURITY CLASSIFICATION OF:			17. LIMITATION OF ABSTRACT	18. NUMBER OF PAGES	19a. NAME OF RESPONSIBLE PERSON
a. REPORT	b. ABSTRACT	c. THIS PAGE			19b. TELEPHONE NUMBER *(include area code)*
U	U	U	UU	50	USAMRMC

TABLE OF CONTENTS

INTRODUCTION

Prostate cancer is the most common malignancy in men and the second leading cause of cancer-related death. Although the use of PSA screening has led to more frequent detection of early disease that can be managed with surgery and/or hormonal therapy (androgen ablation), the development of androgen-independent disease is still a major clinical challenge, and no current therapeutic approach has demonstrated efficacy in this setting. Therefore, there is a critical need for novel therapeutic approaches that will be effective in androgen-independent prostate cancer. Current research is aimed at defining the biological mechanisms underlying androgen independence with the expectation that this information will identify new targets for therapeutic intervention.

We have been studying the effects of proteasome inhibitors in preclinical models of human prostate cancer for almost a decade. Our early work demonstrated that these agents are capable of inhibiting the inflammation-associated transcription factor, NFκB, and bypassing some of the molecular mechanisms implicated in androgen-independent tumor cell survival (for example, overexpression of BCL-2) (1, 2). These observations prompted the initiation of the first-in-man Phase I clinical trial of one of these agents (PS-341, also known as bortezomib or Velcade) in men with androgen-independent prostate cancer, where it displayed promising clinical activity and produced biological effects consistent with NFκB inhibition (suppression of IL-6 production) (3, 4). Based on these promising data a Phase II trial of bortezomib plus mitoxantrone was recently performed at our institution in men with androgen-independent prostate cancer, where even better effects were observed (A. Siefker-Radtke, personal communication). We also demonstrated that proteasome inhibitors block tumor angiogenesis by suppressing VEGF expression (5), and in the course of the past year we have uncovered the molecular mechanisms involved (see below). Finally, in studies that served as the basis for the present project, we discovered that proteasome inhibitors synergize with the pro-apoptotic cytokine, tumor necrosis factor-related apoptosis-inducing ligand (TRAIL), to induce rapid and extensive apoptosis in all human prostate cancer cells and many other solid tumor cell types (6-8). Analysis of the molecular mechanisms involved strongly suggested again that NFκB inhibition was not involved in TRAIL sensitization, contrary to our expectations. Rather, TRAIL sensitization appeared to be related to PS-341-induced cell cycle arrest, and more specifically to p21 accumulation, since chemical inhibitors of cyclin-dependent kinases mimicked the effects of bortezomib, and siRNA-mediated knockdown of p21 attenuated cell death (7). More recent work by other groups has confirmed that p21 promotes TRAIL sensitization (9), but other groups have argued that p21 inhibits cell death (10).

However, in work supported by this grant, we now have data that suggest that the effects of p21 on TRAIL may be unrelated to cell cycle arrest. First, direct transfection with p21 did not enhance TRAIL sensitivity in LNCaP-Pro5 cells, even though it blocked cell cycle progression (K. Zhu, unpublished). Furthermore, siRNA-mediated silencing of cdk1, cdk2, or both kinases also failed to promote TRAIL sensitivity in the cells (K. Zhu, unpublished). We now suspect that bortezomib promotes TRAIL sensitivity by activating an intracellular program known as the unfolded protein response (UPR), a coordinated mechanism that promotes cell survival and/or death in response to endoplasmic reticular (ER) stress (11). A central component of the UPR is the suppression of global protein synthesis (11), and inhibitors of protein or mRNA synthesis are known to reverse cellular resistance to death receptor-mediated apoptosis in other model systems (12). We also suspect that ER stress mediates the effects of bortezomib on cellular DR5 expression (Task 2) via induction of the transcription factor, GADD153 (also known as CHOP) (13). The UPR, and specifically phosphorylation of eIF2α, contributes to the inhibition of VEGF production observed in prostate cancer cells exposed to proteasome inhibitors, and we have obtained solid evidence that this eIF2α phosphorylation also activates a cell death mechanism known as autophagy in prostate cancer cells (see below). Thus, our recent studies have prompted us to redirect focus away from the cell cycle effects of bortezomib to its effects on autophagy, the UPR and ER stress as candidate mediators of TRAIL sensitization. We suspect that we may be able to reinterpret the results we obtained with cdk inhibitors or p21 silencing within this new context.

BODY

Statement of Work

Task 1: To examine the roles of cell cycle arrest and changes in FADD phosphorylation and localization in bortezomib-mediated TRAIL sensitization. **(Months 1-24)**

Task 2: To evaluate the importance of bortezomib-induced upregulation of DR5 and define the molecular mechanisms involved. **(Months 12-30)**

Task 3: To assess the efficacy and potential toxicity of combined therapy with bortezomib plus TRAIL in orthotopic human prostate cancer xenografts. **(Months 1-36)**

Progress

Task 1: We obtained a second clinically relevant proteasome inhibitor (NPI-0052) from Nereus Pharmaceuticals, Inc (San Diego, CA). The compound has several features that may make it superior to bortezomib, including its potency, its distinct spectrum of effects on the 3 proteolytic activities of the proteasome, its oral availability, and its irreversibility (bortezomib is a reversible inhibitor) (14, 15). Like bortezomib, NPI-0052 inhibits cell cycle progression and stabilizes p53 and p21, and it is a potent TRAIL-sensitizing agent (K. Zhu, A. Metwalli, unpublished observations).

As discussed above, we have obtained good evidence that p21-mediated cell cycle arrest is insufficient to promote TRAIL sensitivity in human prostate cancer cells. Furthermore, in parallel studies we used phospho-specific antibodies to determine the role of FADD phosphorylation (S194) (16) in bortezomib-induced TRAIL sensitization. We consistently observed a very modest increase in FADD phosphorylation in cells exposed to either bortezomib alone or bortezomib plus TRAIL (S. Williams, K. Zhu, D.J. McConkey, unpublished observations).

The proteasome plays an essential role in mediating the degradation of misfolded, oxidized, or aggregated proteins (17). When this material accumulates excessively, it activates a coordinated cellular response known as the unfolded protein response (UPR) (17). At the core of the UPR is a protein kinase known as PKR-related ER kinase (PERK) that phosphorylates the eIF2α translational initiation factor, thereby suppressing the translation of most transcripts and reducing protein synthetic burden (11, 17). Because inhibitors of protein or mRNA synthesis are known to promote TRAIL-mediated apoptosis (9), proteasome inhibitor-induced activation of the UPR could explain the TRAIL sensitization we observe in human prostate cancer cells exposed to bortezomib or NPI-0052 plus TRAIL.

We have completed a study that documents that proteasome inhibitors have heterogeneous effects on the UPR in human prostate cancer cells (Zhu et al, manuscript attached and submitted to J. Biol. Chem.). In LNCaP and PC-3 they induce phosphorylation of eIF2α and attenuate protein synthesis, whereas in DU-145 cells (and in 253J B-V bladder cancer cells) they do not. These differences in eIF2α phosphorylation correlate directly with whether or not PIs downregulate HIF-1α, and knockdown of eIF2α in LNCaP or PC-3 cells blocks PI-induced downregulation of HIF-1α. Finally, we used mouse embryonic fibroblasts (MEFs) expressing wild-type (51SS) or a phosphorylation-deficient mutant form of eIF2α (51AA) to directly examine the relationship between PI-induced eIF2α phosphorylation and the observed effects on HIF-1α. PIs induced very modest upregulation of HIF-1α in the wild-type cells but induced strong HIF-1α accumulation in the mutant cells, establishing a cause-effect relationship beween the two. Together, these results establish that PI-induced phosphorylation of eIF2α cause HIF-1α downregulation and mediates the suppression of VEGF production observed in the cells.

The observation that PIs downregulate HIF-1α was paradoxical, since VHL- and proteasome-mediated degradation is crucial in maintaining low level HIF-1α expression in normal cells. The effects of PIs were not limited to preventing HIF-1a translation since they also stimulated downregulation of HIF-1a in cells that had

been preincubated with cobalt chloride to induce HIF-1α accumulation. We therefore wondered whether an alternative proteolytic system might be responsible for HIF-1α downregulation in LNCaP and PC-3 cells. The proteasome and lysosomes are considered to be the two major proteolytic systems responsible for bulk protein turnover in cells. Recent work has established that the two pathways are linked through autophagy (18-23).

We confirmed that PI-mediated downregulation of HIF-1α is blocked by chemical inhibitors of autophagy in prostate cancer cells **(Figure 1).** Furthermore, we have discovered a direct functional link between proteasome inhibition and autophagy, in that PIs induce increased expression of the mRNAs encoding two critical regulators of autophagy (ATG5 and ATG7) in prostate cancer cells **(Figure 2 and data not shown).** Importantly, these effects are mediated via eIF2α phosphorylation, because MEFs expressing the phosphorylation-deficient form of the protein (51AA) fail to display upregulation of ATG5 **(Figure 3).** Finally, our preliminary data indicate that exposure of prostate cancer cells to PIs plus chemical autophagy inhibitors or siRNAs directed against ATG5 or ATG7 enhances cell death **(Figure 4).**

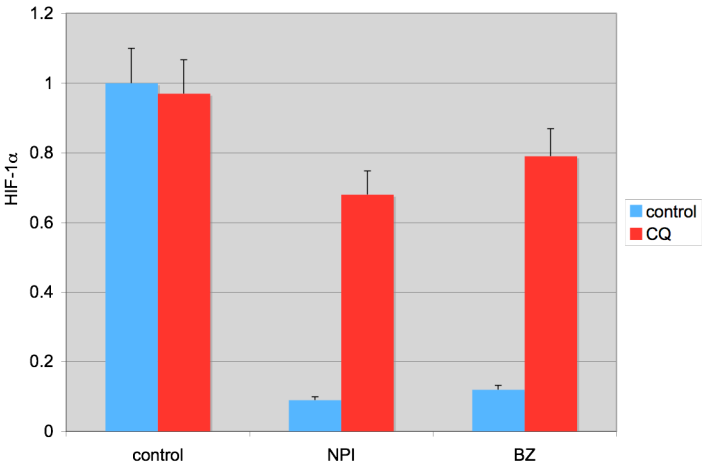

Fig. 1: Effects of the autophagy inhibitor hydroxychloroquine (CQ) on PI-induced downregulation of HIF-1α. Cells were preincubated with CoCl2 overnight before exposing them to 100 nM NPI-0052 or borezomib with or without 50 μM CQ for 8 h, and HIF-1a expression was measured by immunoblotting and densitometry (actin served as a loading control). Mean ± SD, n = 3.

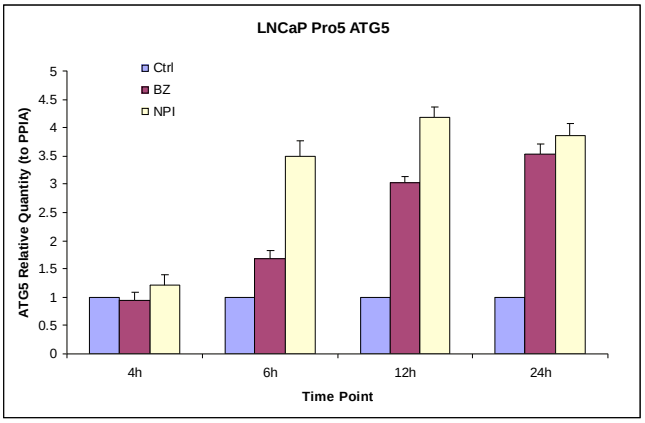

Fig. 2: Effects of PIs on ATG5 mRNA expression in LNCaP-Pro5 cells. Cells were incubated with 100 nM bortezomib (BZ) or 100 nM NPI-0052 for the times indicated, RNA was isolated, and ATG5 levels were measured by real-time quantitative PCR. Mean ± SD, n = 3.

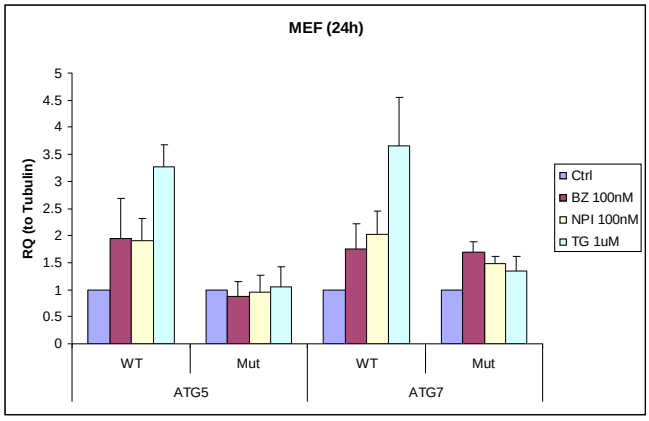

Fig. 3: Effects of PIs or thapsigargin (positive control) on ATG5 expression are phospho-eIF2α-dependent. MEFS were incubated with 100 nM bortezomib (BZ), 100 nM NPI-0052, or 1 μM thapsigargin for 24, and ATG5 and ATG7 levels were measured by real-time PCR. Mean ± SD, n = 3.

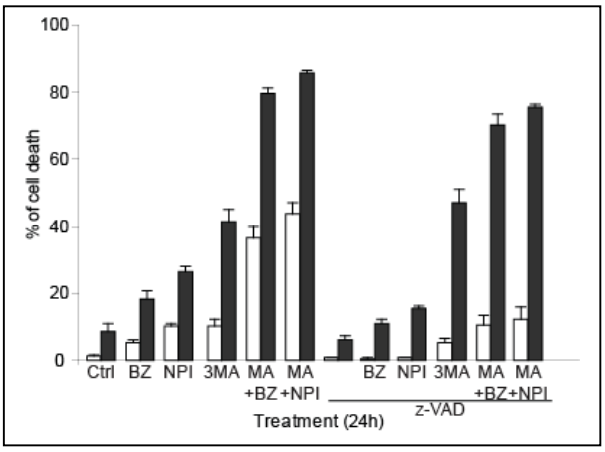

Fig. 4: Effects of the autophagy inhibitor 3-methyladenine (3-MA) on PI-induced cell death. Cells were incubated with 100 nM bortezomib (BZ) or 100 nM NPI-0052 with or without 3-methyladenine (3-MA) for 24 h, and cell death was measured by propidium iodide staining and FACS analysis. Open bars: apoptosis; filled bars, apoptosis plus necrosis. Mean ± SD, n = 3.

Task 2: Several transcription factors are upregulated by the UPR (11, 17). Of these, GADD153/CHOP has been most consistently implicated in cell death (11). We performed preliminary experiments with bortezomib and several other agents that activate the UPR in prostate cancer cells via independent mechanisms, and found that they all increase surface DR5 expression (K. Zhu, unpublished observations), consistent with observations made by another group with prostate cancer cells (24). Another group implicated CHOP in ER stress-mediated upregulation of DR5 in ovarian cancer cells (13).

We have obtained agonistic anti-DR4 and –DR5 antibodies from Human Genome Sciences, Inc (Rockville, MD) and Amgen, Inc (Thousand Oaks, CA). We have performed preliminary studies with them in vitro and have confirmed that exposure of PC-3 cells to a combination of anti-DR5 antibody (plus Protein G as a crosslinker) and NPI-0052 induces strong increases in apoptosis **(Figure 5).** The agonistic antibodies have more desirable pharmacokinetic properties than recombinant TRAIL does in vivo, and the ones we are working with are all in Phase I or II clinical trials, which means that translating our observations into the clinic should be feasible.

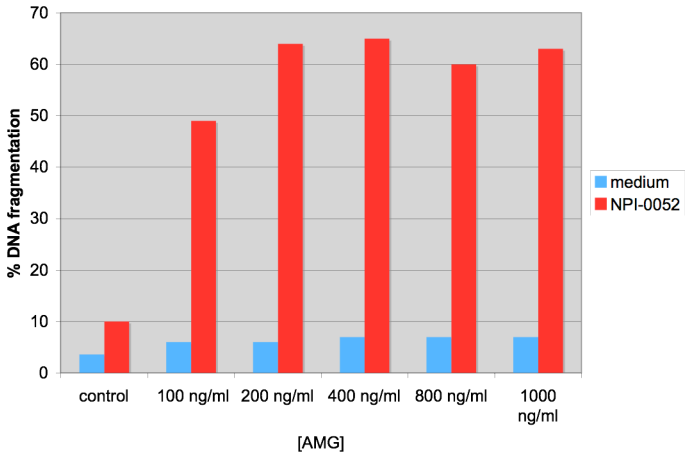

Fig. 5: Effects of an agonistic anti-DR5 antibody on apoptosis in PC-3 cells. Cells were incubated with 100 nM NPI-0052 and the indicated concentrations of AMG-655 (with protein G as a crosslinker) for 24 h, and DNA fragmentation was measured by PI/FACS. Mean results of 2 expts.

Plans for the coming year: We will finish characterizing the effects of PIs on ATG5, ATG7, and autophagy in the prostate cancer cells, with emphases on defining the transcription factor(s) involved in ATG5/7 upregulation and examining the effects of combining PIs and autophagy inhibitors on tumor growth and normal tissue toxicity in mice bearing human prostate cancer xenografts in vivo. We will also perform experiments to examine whether or not the observed synergy between PIs and TRAIL or agonistic anti-TRAIL receptor antibodies involves components of the UPR, including eIF2a phosphorylation, and we will investigate the possible role of p21 in promoting autophagy. Finally, we will finish our studies examining the effects of PIs and other ER stress inducers on apoptosis induced by the agonistic anti-DR4 and anti-DR5 antibodies and the molecular mechanisms leading to DR5 upregulation. We would expect that cells will be especially sensitive to the latter, which could have important implications for future combination studies with these agents.

Task 3: We have performed a number of different toxicity studies in normal and tumor-bearing mice. We treated mice daily with recombinant human TRAIL (prepared in the laboratory)(10 mg/kg, 5x/week), biweekly with bortezomib (1 mg/kg), or both drugs for up to 5 weeks. All of the mice (5 per group) survived therapy and displayed minimal weight loss. Therefore, it appears that a biologically effective dose of TRAIL can be administered with an MTD dose of bortezomib without excessive toxicity.

In preparation for our xenograft studies, we stably transduced LNCaP-Pro5 and PC-3M cells with a lentiviral luciferase construct. These cells were recently implanted into the prostate glands of nude mice, and in vivo tumor burden was measured by luciferase imaging. Unfortunately, the LNCaP-Pro5 tumors did not grow well and they are being "recycled" by reintroduction back into mouse prostates to improve tumor take. However, the PC-3 tumors grew well and are being "recycled" to improve volume reproducibility in preparation for therapy studies. Finally, we have been working with our Prostate SPORE (Nora Navone) to develop primary prostate cancer xenografts that can be used as additional models for this project. In a separate DoD-sponsored project Dr. Ju-Seog Lee (MD Anderson) has begun performing whole genome mRNA profiling on the xenografts (mouse and human arrays), and we are performing preliminary studies to determine how reliable the models are in terms of tumorigenicity and growth over time.

Plans for the coming year: We will perform a therapy study with orthotopic, luciferase-transduced PC-3 tumors within the next 3 months. In this study we will first compare the effects of combination therapy with the PI bortezomib with or without recombinant human TRAIL (10 mpk daily x5) or Amgen's anti-DR5 antibody (10 mg/kg once weekly) on established tumors. As a control, we will also treat mice with docetaxel with or without TRAIL or the antibodies, since taxanes can also dramatically increase TRAIL sensitivity (25) and are frequently used in prostate cancer therapy. Depending on the results, we will then perform the same kinds of experiments with LNCaP-Pro5 tumors or the primary tumor xenografts to determine the degree of inter-tumoral heterogeneity observed in terms of response, and we will use Ju-Seog's datasets to try to determine if there are signature(s) that can be used to understand the basis for such heterogeneity. Finally, we will compare the effects of bortezomib to those of NPI-0052 to assess whether or not one PI is more active than the other.

We have initiated a collaboration with Arlene Siefker-Radtke, a medical oncologist in the Department of Genitourinary Medical Oncology, and Dr. Zhengxin Wang, a basic scientist in the Department of Cancer Biology, to accelerate research progress within this project. Dr. Wang is studying the molecular mechanisms that regulate expression of the TRAIL receptor inhibitor c-FLIP in prostate cancer cells, and Dr. Siefker-Radtke has been performing clinical trials with PIs in patients with androgen-independent disease. Our plan is to pool our expertise in order to define how TRAIL-induced apoptosis is regulated by androgen receptor and other signaling pathways, to identify the "best" combination of TRAIL or agonistic anti-TRAIL receptor antibody in our preclinical models, and then to perform a clinical trial with the "best" combination in patients. Our industry partners have stated that they are interested in supporting such a trial.

KEY RESEARCH ACCOMPLISHMENTS

- Showed for the first time that proteasome inhibitors activate the UPR in some (but not all) human prostate cancer cells.
- Showed that proteasome inhibitors downregulate HIF-1α in the same cells
- Obtained preliminary evidence that c-FLIP downregulation is important for TRAIL sensitization in PC-3 cells
- Obtained preliminary evidence that proteasome inhibitors activate autophagy in prostate cancer cells, and autophagy mediates the elimination of HIF-1a protein in the cells
- Obtained preliminary evidence that ER stress upregulates DR5 expression in prostate cancer cells
- Determined that mice tolerate therapy with proteasome inhibitors plus TRAIL

REPORTABLE OUTCOMES

- Manuscript describing the effects of proteasome inhibitors on the UPR submitted to J. Biol. Chem.
- Manuscript describing the effects of PIs on autophagy in preparation
- Generated LNCaP-Pro5 and PC-3M cells stably transduced with luciferase

CONCLUSIONS

- Phosphorylation of eIF2α couples proteasome inhibition to HIF-1α suppression and autophagy

- The effects of proteasome inhibitors on specific components of the UPR (eIF2α phosphorylation in particular) are heterogeneous, and this may be important to the development of mechanism-based combination therapies
- Agonstic antibodies synergize with PIs to induce apoptosis in human prostate cancer cells in vitro, but a crosslinking agent (protein G) is required

REFERENCES

1. Bold RJ, Virudachalam S, McConkey DJ. Chemosensitization of pancreatic cancer by inhibition of the 26S proteasome. J Surg Res 2001;100:11-7.
2. Nawrocki ST, Bruns CJ, Harbison MT, et al. Effects of the proteasome inhibitor PS-341 on apoptosis and angiogenesis in orthotopic human pancreatic tumor xenografts. Mol Cancer Ther 2002;1:1243-53.
3. Papandreou CN, Daliani DD, Nix D, et al. Phase I trial of the proteasome inhibitor bortezomib in patients with advanced solid tumors with observations in androgen-independent prostate cancer. J Clin Oncol 2004;22:2108-21.
4. Papandreou CN, Logothetis CJ. Bortezomib as a potential treatment for prostate cancer. Cancer Res 2004;64:5036-43.
5. Williams S, Pettaway C, Song R, Papandreou C, Logothetis C, McConkey DJ. Differential effects of the proteasome inhibitor bortezomib on apoptosis and angiogenesis in human prostate tumor xenografts. Mol Cancer Ther 2003;2:835-43.
6. Papageorgiou A, Lashinger L, Millikan R, et al. Role of tumor necrosis factor-related apoptosis-inducing ligand in interferon-induced apoptosis in human bladder cancer cells. Cancer Res 2004;64:8973-9.
7. Lashinger LM, Zhu K, Williams SA, Shrader M, Dinney CP, McConkey DJ. Bortezomib abolishes tumor necrosis factor-related apoptosis-inducing ligand resistance via a p21-dependent mechanism in human bladder and prostate cancer cells. Cancer Res 2005;65:4902-8.
8. Khanbolooki S, Nawrocki ST, Arumugam T, et al. Nuclear factor-kappaB maintains TRAIL resistance in human pancreatic cancer cells. Mol Cancer Ther 2006;5:2251-60.
9. Fulda S, Debatin KM. Sensitization for tumor necrosis factor-related apoptosis-inducing ligand-induced apoptosis by the chemopreventive agent resveratrol. Cancer Res 2004;64:337-46.
10. Xu SQ, El-Deiry WS. p21(WAF1/CIP1) inhibits initiator caspase cleavage by TRAIL death receptor DR4. Biochem Biophys Res Commun 2000;269:179-90.
11. Szegezdi E, Logue SE, Gorman AM, Samali A. Mediators of endoplasmic reticulum stress-induced apoptosis. EMBO Rep 2006;7:880-5.
12. Fulda S, Meyer E, Debatin KM. Metabolic inhibitors sensitize for CD95 (APO-1/Fas)-induced apoptosis by down-regulating Fas-associated death domain-like interleukin 1-converting enzyme inhibitory protein expression. Cancer Res 2000;60:3947-56.
13. Yamaguchi H, Wang HG. CHOP is involved in endoplasmic reticulum stress-induced apoptosis by enhancing DR5 expression in human carcinoma cells. J Biol Chem 2004;279:45495-502.
14. Chauhan D, Catley L, Li G, et al. A novel orally active proteasome inhibitor induces apoptosis in multiple myeloma cells with mechanisms distinct from Bortezomib. Cancer Cell 2005;8:407-19.
15. Ruiz S, Krupnik Y, Keating M, Chandra J, Palladino M, McConkey D. The proteasome inhibitor NPI-0052 is a more effective inducer of apoptosis than bortezomib in lymphocytes from patients with chronic lymphocytic leukemia. Mol Cancer Ther 2006;5:1836-43.
16. Scaffidi C, Volkland J, Blomberg I, Hoffmann I, Krammer PH, Peter ME. Phosphorylation of FADD/ MORT1 at serine 194 and association with a 70-kDa cell cycle-regulated protein kinase. J Immunol 2000;164:1236-42.
17. Kaufman RJ. Orchestrating the unfolded protein response in health and disease. J Clin Invest 2002;110:1389-98.
18. Ding WX, Ni HM, Gao W, et al. Linking of autophagy to ubiquitin-proteasome system is important for the regulation of endoplasmic reticulum stress and cell viability. Am J Pathol 2007;171:513-24.
19. Ding WX, Yin XM. Sorting, recognition and activation of the misfolded protein degradation pathways through macroautophagy and the proteasome. Autophagy 2008;4:141-50.

20. Harada M, Kumemura H, Omary MB, et al. Proteasome inhibition induces inclusion bodies associated with intermediate filaments and fragmentation of the Golgi apparatus. Exp Cell Res 2003;288:60-9.
21. Pandey UB, Nie Z, Batlevi Y, et al. HDAC6 rescues neurodegeneration and provides an essential link between autophagy and the UPS. Nature 2007;447:859-63.
22. Rubinsztein DC. Autophagy induction rescues toxicity mediated by proteasome inhibition. Neuron 2007;54:854-6.
23. Yang W, Monroe J, Zhang Y, George D, Bremer E, Li H. Proteasome inhibition induces both pro- and anti-cell death pathways in prostate cancer cells. Cancer Lett 2006;243:217-27.
24. Johnson TR, Stone K, Nikrad M, et al. The proteasome inhibitor PS-341 overcomes TRAIL resistance in Bax and caspase 9-negative or Bcl-xL overexpressing cells. Oncogene 2003;22:4953-63.
25. Nimmanapalli R, Perkins CL, Orlando M, O'Bryan E, Nguyen D, Bhalla KN. Pretreatment with paclitaxel enhances apo-2 ligand/tumor necrosis factor-related apoptosis-inducing ligand-induced apoptosis of prostate cancer cells by inducing death receptors 4 and 5 protein levels. Cancer Res 2001;61:759-63.

Phosphorylation of eIF2 downregulates HIF-1 in response to proteasome inhibition

Keyi Zhu[1,2], John V Heymach [1,3] and David J McConkey[1,2]

[1]Departments of Cancer Biology and [2]Urology and [3]Thoracic/Head and Neck Oncology, The University of Texas M.D. Anderson Cancer Center, Houston, Texas 77030

Running title: Regulation of HIF-1α by the UPR

Key words: Bortezomib, NPI-0052, VEGF, ER stress, prostate cancer

Address correspondence to:

David McConkey

Departments of Urology and Cancer Biology

U.T. M.D. Anderson Cancer Center

1515 Holcombe Boulevard

Houston, Texas 77030

Tel. (713) 792-8591

Email: dmcconke@mdanderson.org

SUMMARY

Hypoxia inducible factor 1α (HIF-1α) plays a central role in regulating tumor angiogenesis via its effects on VEGF transcription, and its expression is regulated through proteasome-mediated degradation. Paradoxically, previous studies have shown that proteasome inhibitors (PI) block tumor angiogensis by reducing vascular endothelial growth factor (VEGF) expression, but the mechanisms have not been identified. Here we show that proteasome inhibitors downregulate HIF-1α protein levels and block HIF-1α's transcriptional activity in human prostate cells. HIF-1α downregulation was associated with PI-mediated phosphorylation of the translation initiation factor eIF2alpha and inhibition of translation and was also observed in cells exposed to thapsigargin and tunicamycin, two conventional inducers of endoplasmic reticular (ER) stress that also induce phosphorylation of eIF2α. Interestingly, PIs failed to induce eIF2α phosphorylation or translational attenunation in DU145 or 253JB-V cells and in these cells PIs induced HIF-1α accumulation. Futhermore, PIs induced HIF-1α accumulation in LNCaP Pro5 cells depleted of eIF2α via siRNA transfection. Finally, PIs stimulated marked over-accumulation of HIF-1alpha in knock-in MEFs expressing a phosphorylation-deficient mutant form of eIF2alpha (eIF2α$^{51A)}$ compared to wild-type controls. Our data establish that PIs downregulate HIF-1α expression in cells that display UPR activation by stimulating eIF2α phosphorylation.

INTRODUCTION

The 26S proteasome is a large, multicatalytic enzyme that functions as one of the major routes of intracellular protein degradation (1,2). Its substrates include cell cycle intermediates and direct and indirect regulators of apoptosis, and several different PIs have been developed for use in cancer therapy. Bortezomib (PS-341, also known as Velcade®, Millennium Pharmaceuticals, Inc.) is a peptide boronate inhibitor of the chymotryptic activity of the proteasome that received FDA approval for the treatment of multiple myeloma (MM) and mantle cell lymphoma (MCL) (1-4). Its clinical success

has prompted other companies to develop chemically distinct PIs that might make them even more active. One such compound is NPI-0052 (*salinosporamide* A, Nereus Pharmaceuticals), a structural analog of the proteasome inhibitor lactacystin that is currently being evaluated in phase I clinical trials. NPI-0052 is orally bioactive, irreversible, and has broader proteasome inhibitory activity than bortezomib (5,6).

Analyses of the direct cytotoxic effects of PIs in tumor cells have identified a number of different biochemical mechanisms, including inhibition of pro-survival transcription factor nuclear factor kappaB (NFκB), accumulation of pro-apopototic proteins, like p53, Bax, Bik and NOXA (7-11), and endoplasmic reticular (ER) stress (refs). However, other studies showed that proteasome inhibitors also suppress angiogenesis by downregulating vascular endothelial growth factor (VEGF) expression (5,12,13). Tumor VEGF expression is controlled in large part by the transcription factor, HIF-1 (14-16). HIF-1 is a heterodimer composed of an O_2 sensitive alpha subunit (HIF-1) and a constitutively expressed beta subunit (HIF-1β/ARNT) (14,17,18). Under normoxic conditions, HIF-1 is hydroxylated at two proline residues (P402 and P564) by prolyl hydroxylase-domain proteins (PHD) and is subsequently recongnized by Von Hippel-Lindau (VHL), a component of an E3 ubiquitin-protein ligase that targets HIF-1α for degradation by the proteasome (14,18,19). Under hypoxic conditions HIF-1 is not hydroxylated and it accumulates. Loss of VHL expression is a common feature of renal cell carcinoma and it results in overexpression of VEGF and increased angiogenesis (refs). Overexpression of HIF-1 has been observed in many other solid tumors, including prostate, breast, lung and head and neck cancers, and chemical inhibitors of HIF-1 are being developed for cancer therapy (14,18,20,21).

We were struck by the paradox that HIF-1a expression is controlled primarily by the proteasome yet PIs downregulate VEGF expression. We therefore initiated the present study to characterize the effects of PIs on HIF-1a function. Here we report that bortezomib and NPI-0052 selectively blocked HIF-1 's expression and activity in a subset of human prostate cancer cells. Analyses of the biochemical mechanisms involved revealed that they involved processes observed during ER stress including

phosphorylation of the translation initiation factor eIF2a on a specific serine residue (S51) that also resulted in suppression of protein synthesis. Similar effects were observed in cells exposed to other stimuli that induce ER stress and stimulate eIF2a phosphorylation, indicating that the response may have broader biological significance.

Experimental Procedures

Cell lines and culture

Human LNCaP Pro5 cells, derived via orthotopic recycling of LNCaP prostate cancer cells, were generously provided by Dr. Curtis Pettaway (Department of Urology, University of Texas M.D. Anderson Cancer Center). Human PC-3 and DU-145 prostate cancer cells were obtained from American Type Culture Collection (Rockville, MD). 253JB-V bladder cancer cells were generated via orthotopic recycling of the 253JP human TCC (Transitional Cell Carcinoma) bladder cell line and were provided by Dr. Colin Dinney (Department of Urology, University of Texas M.D. Anderson Cancer Center). eIF2 ^{Ser51SS} wild type and eIF2 ^{Ser51AA} knock-in mutant mouse embryonic fibroblast cells (MEFs) were kindly provided by Dr. David Ron (New York University School of Medicine, NY). The prostate cancer cells were grown in RPMI 1640 (Life Technologies, Inc., Gaithersburg, MD) supplemented with 10% fetal bovine serum (Life Technologies), 1% vitamins (Life Technologies), sodium pyruvate (Bio Whittaker, Rockland, ME), L-glutamine (Bio Whittaker), penicillin/streptomycin solution (Bio Whittaker), and non-essential amino acids (Life Technologies) under conditions of 5% CO_2 at 37°C in an incubator. 253JB-V cells were cultured in MEM media containing the same supplements. The MEF cells were grown in dMEM supplemented with 10% fetal bovine serum, 1% penicillin/streptomycin solution, L-glutamine, non-essential amino acids, 55mM -mercaptoethanol. Leucine free media was purchased from MP Biomedicals (Solon, OH) for measuring protein synthesis. For hypoxic exposure, cells were placed in a NAPCO Water-Jacketed CO_2 incubator (Thermo Fisher Scientific, Inc., Waltham, MA) flushed with 0.2% oxygen, 5% CO_2 and 95% nitrogen. Hypoxia was also mimicked by incubating cells with 100 μM of cobalt chloride ($CoCl_2$) in a regular atmosphere.

Reagents, antibodies and plasmids

The proteasome inhibitor bortezomib (PS-341, Velcade) and the IkappaB kinase (IKK)/NFκB inhibitor PS-1145 were provided by Millenium Pharmaceuticals (Cambridge, MA). The proteasome inhibitor NPI-0052 was provided by Nereus Pharmaceuticals (San Diego, CA). Cycloheximde (CHX), thapsigargin (TG), tunicamycin (TM) and cobalt chloride ($CoCl_2$) were purchased from Sigma Chemical Co. (St. Louis, MO). Antibodies were obtained from the following commercial sources: human HIF-1 (BD Biosciences Transduction Laboratories™); mouse HIF-1 , HIF-2 and HIF-1β (Novus Biologicals Inc., Littleton, CO); eIF2 and phosphorylated eIF2 at Ser52 (Invitrogen Biosource™, Carlsbad, CA); phosphorylated eIF2 at Ser51 (Cell Signaling Technology, Inc., Danvers, MA); phosphorylated PERK at Thr851, P300 and Ref-1 (Santa Cruz Biotechnology, Santa Cruz, CA); and anti-actin (Sigma Chemical Co., St. Louis, MO). Horseradish peroxidase (HRP)–conjugated secondary antibodies were obtained from Amersham Pharmacia Biotech (Piscataway, NJ). Hypoxia response element (HRE)-driven *firefly* luciferase plasmid was purchased from Panomics Inc. (Fremont, CA).

Immunoblotting

Cells were lysed for 1 h at 4°C in Triton lysis buffer [1% Triton X-100, 150 mmol/L NaCl, 25 mmol/L Tris (pH 7.5), 1 mmol/L glycerol phosphate, 1 mmol/L sodium orthovanadate, 1 mmol/L sodium fluoride, and one Complete Mini Protease Inhibitor Cocktail tablet (Roche, Indianapolis, IN)]. Lysates were centrifuged for 5 minutes at 12,000×*g* (4°C). Total cellular protein (~20 μg) from each sample was mixed with an equal volume of 2×SDS-PAGE sample buffer (50 mmol/L Tris-HCl, 2% SDS, 0.1% bromophenol blue, 10% glycerol, and 5% β-mercaptoethanol). Samples were then boiled for 5 minutes at 100°C and were resolved by SDS-PAGE. Proteins were transferred to nitrocellulose membranes, and the membranes were blocked with 5% nonfat milk in a TBS solution containing 0.1% Tween-20 or blocked with 5% BSA in TBST solutions (for phosphor-specific antibodies) for 1 h at room temperature. The blots were then probed with

indicated primary antibodies overnight at 4°C, washed with TBST solution, and probed with species-specific secondary antibodies coupled to horseradish peroxidase. Immunoreactive material was detected by enhanced chemiluminescence (West Pico, Pierce, Inc., Rockville, IL). For sequential blotting with additional antibodies, the membranes were stripped using a buffer containing 80 mM Tris-HCl, 2% SDS, 1% β-mercaptoethanol, PH 6.7, at 60°C for 30 minutes and reprobed with the indicated antibodies. Densitometry quantification of proteins levels was performed using ImageJ software [National Institutes of Health (NIH), Bethesda, MD].

Quantification of VEGF by Enzyme-linked immunosorbent assays (ELISA)

LNCaP Pro5 cells (5×10^4 cells/well) were plated in 24-well plates. After 24 h attachment, cells were exposed to 100 nM bortezomib, 100 nM NPI-0052, or 10-20 μM of PS1145 for 24 h under normoxic or hypoxic conditions. Media were then collected and VEGF levels were determined using Quantikine ELISA kits (R&D Systems, Inc., Minneapolis, MN). The results were expressed as concentrations of VEGF (pg/ml) per 5×10^4 cells/well. At these time points the drugs did not produce significant toxicity in the LNCaP Pro5 cells.

Luciferase reporter assays

To examine the transcriptional activity of HIF-1, LNCaP Pro5 cells (5×10^4 cells/well) were plated in 24-well plates. After 24 h, cells were cotransfected with plasmids encoding a *firefly* luciferase reporter driven by a promoter containing an hypoxia responsive element (HRE) and *renilla* luciferase under the control of an autologous promoter (pRL-CMV) (internal control for transfection efficiency) using TransFast (Promega Co., Madison, WI) following the manufacturer's instructions. After exposure to the indicated transfection mixture for 30 h, cells were incubated with 100 nM bortezomib or 100 nM NPI-0052 for the indicated times in normoxic or 0.2% O_2 conditions, and luciferase activity was measured using the Dual-luciferase assay system (Promega Co, Madison, WI). *Firefly* luciferase activity was normalized by *renilla* luciferase activity and the indicated promoter activities were expressed as the average ratios of *firefly* to *renilla* luciferase

activities (±SEM) from at least three independent experiments.

Small interfering RNA–mediated silencing of HIF-1α and eIF2α

LNCaP Pro5 cells were grown to ~60% confluency in 6-well plates and transfected with small interfering RNA (siRNA) targeting human HIF-1 , eIF2 or siRNA nonspecific control for 48 h (Dharmacon RNA Technologies, Lafayette, CO). Liposome-mediated transfection was accomplished using the Oligofectamine reagent according to the manufacturer's protocol (Invitrogen Life Technologies, Carlsbad, CA). Following silencing, cells were incubated as indicated, VEGF expression was measured by ELISA, and HIF-1 expression was examined by immunoblotting. The efficiency of gene silencing was verified in each experiment by immunoblotting.

Quantitative real time-PCR

LNCaP Pro5 cells were grown to ~ 80% confluency in 10 cm dishes and exposed to 100 nM bortezomib or 100 nM NPI-0052. After 12 h incubation under either normoxic or hypoxic conditions, total cellular mRNA was isolated using an RNeasy kit (Qiagen, Valencia, CA) according to the manufacturer's instructions. One microgram of total mRNA was reverse transcribed for 2 h at 37°C in a total of 20 μl mixture using SuperArray First-Strand cDNA Kit (Superarray Bioscience Co., Frederick, MD) following the manufacturer's instructions. Quantitative real time polymerase chain reaction (qPCR) was performed in triplicate. The expression of each target gene was quantified using a Bio-Rad iCycler real-time PCR system (Bio-Rad Laboratories, Inc., Hercules, CA). Each 25 μl reaction mixture consisted of 1.5 μl the first strand cDNA and 0.5 μM each primer, 12.5 μl RT² Real-Time™ SYBR Green/Fluorescein from SuperArray. The following primer pairs were utilized for target gene mRNA amplification: HIF-1, and GAPDH (SuperArray Bioscience Co., Frederick, MD). The amplification protocol consisted of one cycle at 95°C for 3 min, followed by 40 cycles at 95°C for 30 sec, 58°C for 30 sec, then 72°C for 30 sec. The melt-curve protocol, performed at the end of the amplification, consisted of 80 cycles beginning at 55°C for 10 sec, and then the temperature was increased by 0.5°C/cycle. A standard curve for each target gene

was generated to determine the linear range and amplification efficiency. PCR efficiency greater than 80% was considered sufficient. The threshold cycle for each sample was fitted to the standard curve to calculate the expression level of the target gene relative to the input mRNA. The resulting data were analyzed with the iCycler iQ Real-Time Detection System software and expressed as the averages of ratios (relative expression to control) ±SEM.

Quantification of protein synthesis by [$_{L\text{-}4,5\text{-}}^{3}$H]Leucine incorporation

Equal numbers of cells were plated in 6-well plates. After 24 h attachment, cells were incubated with 100 nM bortezomib or 100 nM NPI-0052 for 4 h under normoxic conditions. Cycloheximide (40 μM) and thapsigargin (10 μM) were used as positive controls. At the end of the experiments no significant difference of viable cell numbers were observed between untreated and treated samples. Cells were washed with phosphate-buffered saline (PBS) and trans-labeled with leucine-free medium (MP Biomedicals, Solon, OH) plus [$_{L\text{-}4,5\text{-}}^{3}$H]Leucine [2μCi/ml, GE Healthcare Bio-Sciences Corp. (Piscataway, NJ)] for 2 h at 37°C under normoxic conditions. Excess un-incorporated [$_{L\text{-}4,5\text{-}}^{3}$H]Leucine was removed by washing cells with ice-cold PBS. Cells were collected and lysed as previously described. Equal volumes of cellular protein (~20 μl) from each sample were precipitated by ice cold trichloroacetic acid (TCA, 10%, w/v) at 4°C for 30 min. Precipitated proteins were then dissolved in 100 μl 0.1 M KOH and transferred to vials for scintillation counting to determine the [$_{L\text{-}4,5\text{-}}^{3}$H]Leucine incorporation into proteins.

Data analysis

Experiments presented in the figures are derived from or are representative of at least three independent repetitions. Statistical analyses were performed using GraphPad 3.05 statistical software (GraphPad Software, San Diego, CA) using the Student's *t* test, or one-way ANOVA where appropriate ($P<0.05$ was considered statistically significant).

RESULTS

Bortezomib and NPI-0052 downregulate HIF-1α, HIF-2α and VEGF expression. Bortezomib and NPI-0052 inhibit angiogenesis but the

molecular mechanisms involved remain unclear (1,5,12,13). HIF-1 is considered one of the most important pro-angiogenic transcription factors and its expression is tightly regulated by the ubiquitin/proteasome degradation pathway (14,32). We therefore assessed the effects of proteasome inhibitors on HIF-1 protein accumulation and transcriptional activity in human prostate cancer cells. HIF-1 was almost undetectable under normoxic conditions but was strongly upregulated by exposure to hypoxia or $CoCl_2$ (Figure 1A). Paradoxically, both proteasome inhibitors caused concentration dependent downregulation of HIF-1 in LNCaP Pro5 cells, measured after 12 h drug exposure (Figure 1A). The effects of NPI-0052 were stronger than those of bortezomib at 10 nM, consistent with its greater potency as a proteasome inhibitor (5,6). Proteasome inhibitors also downregulated nuclear HIF-1 protein levels as determined by cell fractionation and immunoblotting (data not shown). HIF-2, which is also regulated via proteasome dependent degradation (14,33), was also downregulated in cells exposed to bortezomib or NPI-0052 (Figure 1A). Since HIF-1 is a transcription factor that drives gene expression via HRE elements, we also investigated whether or not proteasome inhibitors affected the transcriptional activity of HIF-1. PIs reduced HRE-driven luciferase activity under basal and hypoxic conditions in LNCaP Pro5 cells (Figure 1B).

VEGF is transcriptionally regulated via HIF-1α binding to an HRE located in the 5' flanking region of the VEGF promoter (16,32,34,35). To further examine the effects of proteasome inhibitors on HIF-1α transcriptional activity, we measured VEGF levels in the conditioned media obtained from LNCaP Pro5 cells exposed to proteasome inhibitors. Under normoxic conditions, LNCaP Pro5 cells secreted detectable levels of VEGF that were strongly increased by exposure to hypoxia or $CoCl_2$. VEGF expression was inhibited by bortezomib or NPI-0052 in a time-dependent manner (Figure 1C and data not shown). To examine whether proteasome inhibitor-mediated downregulation of VEGF was a result of blocking HIF-1α activity, we used a VEGF reporter construct to measure its transcription. Again, hypoxia promoted VEGF promoter-driven luciferase expression and proteasome inhibitors

blocked these effects, confirming that the suppression of VEGF was associated with inhibition of VEGF transcription (data not shown). We also used siRNA targeting HIF-1α to knock down HIF-1α expression and measured VEGF expression by ELISA. Knockdown of HIF-1α reduced basal and hypoxia-induced VEGF secretion and enhanced the inhibitory effects of proteasome inhibitors on VEGF expression (Figure 1D), confirming that HIF-1α plays a crucial role in regulating VEGF expression in LNCaP Pro5 cells.

The VEGF promoter region contains several distinct *cis*-acting elements, including the HRE as well as binding sites for other transcription factors, such as signal transducer and activator of transcription 3 (STAT3), activating protein–1 (AP-1), AP-2, NFκB, and SP-1 (16,34,36,37). Given the broad substrate spectrum of the proteasome, these factors may all be affected by proteasome inhibitors. Therefore, we examined the effects of proteasome inhibitors on several other VEGF regulators in LNCaP Pro5 cells. We focused on HIF-1β/ARNT, STAT3, P300 and Redox effector factor-1/apurinic/apyrimidinic endonuclease (Ref-1/APE) because these factors form a hypoxia-inducible transcriptional complex with HIF-1α on the VEGF promoter's HRE region. Strikingly, none of these molecules was downregulated by bortezomib or NPI-0052 (Figure 2A), although the results do not rule out the possibility that their binding to the VEGF promoter was disrupted by the PIs. We also examined the potential role of NFκB in the proteasome inhibitor mediated suppression of VEGF expression since proteasome inhibitors were originally designed to inhibit NFκB activity via stabilization of IκBα. To this end, we examined the effects of the IKK inhibitor, PS-1145, on VEGF expression. PS-1145 had no effects on VEGF expression at biologically active concentrations under normoxic or hypoxic conditions (Figure 2B), even though NFκB activity was inhibited at these doses as measured by NFB EMSA (electrophoretic mobility shift assay) (9,38). Therefore, our data strongly suggest that the effects of proteasome inhibitors on VEGF expression are not linked to suppression of NFB activity.

Effects of proteasome inhibitors on HIF-1α mRNA levels. To determine whether or not the downregulation of HIF-1 induced by proteasome inhibitors occurred at the transcriptional level, we exposed LNCaP Pro5 cells to bortezomib or NPI-0052 and performed quantitative HIF-1 RT-PCR (Figure 3A). The summary data (from three independent experiments) demonstrated that hypoxia did not upregulate HIF-1α mRNA expression after 12 h and proteasome inhibitors had no measurable effects on HIF-1α mRNA levels at this time point under either conditions tested (normoxia: Ctrl, 1 ± 0.06; bortezomib, 0.92 ± 0.09; NPI-0052, 1.11 ± 0.11. hypoxia: Ctrl, 1 ± 0.21; bortezomib, 1.02 ± 0.25; NPI-0052, 1.12 ± 0.17). The specificities of the amplified products were confirmed by melting curve analyses and gel electrophoresis (data not shown). The levels of GAPDH were used as an internal control to evaluate the amount of starting material for each sample. No significant differences in GAPDH mRNA levels were observed in any of the samples.

Biphasic effects of proteasome inhibitors on HIF-1α's half-life. As discussed above, the expression of HIF-1α is tightly controlled via VHL-directed proteasomal degradation. Therefore, we examined the effects of proteasome inhibitors on HIF-1α stability by immunoblotting using cellular extracts prepared from cells incubated with the protein translation inhibitor cycloheximide (CHX). LNCaP Pro5 cells were pre-incubated with $CoCl_2$ for 16 h to stimulate HIF-1α accumulation and then exposed to proteasome inhibitors with or without CHX. Levels of HIF-1α were detectably lower in CHX-exposed cells as compared to controls at 30 min and were almost undetectable by 2 h. In cells exposed to CHX plus proteasome inhibitors, levels of HIF-1 were about 60% higher than the levels observed in cells exposed to CHX alone at 30 min, although by 2 h HIF-1 levels were significantly reduced (Figure 3B). In cells exposed to proteasome inhibitor alone, HIF-1α accumulation was also observed at 30 min (~50% induction compared to control), but HIF-1α protein levels returned to control levels by 1 h and then decreased. As shown in Figure 3B, bortezomib

and NPI-0052 downregulated HIF-1α so rapidly that there was almost no detectable HIF-1α in cells exposed to the proteasome inhibitors with or without CHX by 4 h. Based on these observations, we conclude that proteasome inhibitors have biphasic effects on HIF-1, causing an early accumulation of HIF-1 followed by profound downregulation of protein expression. Importantly, both proteasome inhibitors cause sustained proteasome inhibition in the same cells (>24 h) and other labile proteins do in fact accumulate in the cells at 4 h and later (Figure 4D and (10,12,39)).

Effects of proteasome inhibitors on the UPR and eIF2α dependent protein translation in human cancer cells. Recent studies have demonstrated that proteasome inhibitors induce a terminal ER stress in cancer cells (11,22,24,25). Cells have evolved protective mechanisms that are collectively termed the "unfolded protein response" to alleviate ER stress or induce apoptosis if the stress is excessive. PERK/eIF2α has been implicated in the UPR that activation of PERK results in phosphorylation of eIF2α and subsequent attenuation of protein synthesis. Meanwhile, eIF2α phosphorylation selectively induces the translation of activating transcription factor 4 (ATF4) and its downstream transcriptional targets (23,27,28,40,41). Considering that the short-lived proteins are very sensitive to translational regulation, we hypothesized that proteasome inhibitor-mediated translational repression might contribute to the downregulation of HIF-1α observed in the LNCaP Pro5 cells. To test this, we first examined the effects of proteasome inhibitors on PERK and eIF2α phosphorylation and protein synthesis. Bortezomib and NPI-0052 induced PERK phosphorylation at Thr981. The classic ER stress inducer, thapsigargin (TG, which inhibits the sarcoplasmic/endoplasmic Ca^{2+}-ATPase SERCA) also induced PERK phosphorylation (Figure 4A). Both proteasome inhibitors induced eIF2 phosphorylation at Ser52 as detected by immunoblotting under normoxic and hypoxic conditions in LNCaP Pro5 cells (Figure 4B). Hypoxia itself induced eIF2α phosphorylation, consistent with other studies implicating PERK and eIF2 in the adaptation response to hypoxia

(27,40,42). PI-induced phosphorylation of eIF2α was associated with inhibition of protein synthesis as measured by [$_{L\text{-}4,5\text{-}}^{3}$H]Leucine incorporation (Figure 4C). The inhibitory effects on protein synthesis lasted for at least 12 h and were not associated with cell death (data not shown). Furthermore, thapsigargin and another classic ER stress inducer tunicamycin (TM, which inhibits N-linked protein glycosylation) downregulated HIF-1α (Figure 4D). We have also obtained data showing that proteasome inhibitors induce accumulation of ATF4 (data not shown). Our results are consistent with previous data implicating the UPR in the effects of PIs, but it is also possible that UPR-independent mechanisms are involved as well.

Cell line-dependent effects of proteasome inhibitors on eIF2alpha phosphorylation and HIF-1α accumulation. Proteasome inhibitor-mediated phosphorylation of eIF2alpha has been reported in several tumor models, but in others proteasome inhibitors have been shown to block eIF2α phosphorylation (22-25). Therefore, we characterized the effects of proteasome inhibitors on eIF2α phosphorylation and HIF-1α protein levels in three additional genitourinary cancer cell lines. In PC3 prostate cancer cells, both PIs induced eIF2α phosphorylation and global translation repression, and these effects were associated with HIF-1α downregulation (Figure 5). In contrast, both drugs failed to induce phosphorylation of eIF2α or inhibit protein synthesis in DU145 or 253JB-V cells, and they actually promoted the accumulation of HIF-1 in both cell lines (Figure 5). Therefore, the effects of proteasome inhibitors are heterogeneous, and downregulation of HIF-1 only occurs in cells that display proteasome inhibitor induced eIF2 phosphorylation and protein translation repression.

Effects of eIF2α regulation on HIF-1α protein level. The correlation between eIF2α phosphorylation and HIF-1α downregulation suggested that the two events might be mechanistically linked. Therefore, we examined the levels of HIF-1 in LNCaP Pro5 cells transfected with siRNA specific for eIF2 or an off-target control construct. Strikingly,

bortezomib and NPI-0052 induced the accumulation of HIF-1 in cells depleted eIF2α, and similar effects were observed in cells exposed to thapsigargin (Figure 6A). Knocking down eIF2 partially reversed PI-induced protein translation attenuation (Supplemental Figure 1A). We next compared the effects on HIF-1 of proteasome inhibitors in mouse embryonic fibroblast cells expressing wild type (eIF2 ^{51SS}) or a phosphorylation-deficient mutant (eIF2 ^{51AA}) form of eIF2 . Consistent with the results in the prostate and bladder cancer cells, the strong eIF2 phosphorylation induced by PIs in the wild-type MEFs was associated with modest accumulation of HIF-1, while PIs induced strong HIF-1 accumulation in the phosphorylation-deficient mutant cells. Direct measurements of PI-mediated translational suppression in the two cells confirmed that it was dependent on eIF2 phosphorylation (Figure 6B & 6C). Altogether, these data demonstrate that the downregulation of HIF-1 induced by PIs is mediated by eIF2 phosphorylation and is linked to translational repression.

DISCUSSION

The proteasomal degradation pathway is thought to mediate the destruction of the vast majority of cellular proteins to maintain intracellular homeostasis and cell function, and proteasome inhibition has been validated as an effective therapeutic strategy for certain hematological tumors. We have shown previously the antitumoral effects of bortezomib are associated with suppression of VEGF expression and angiogenesis. In the past PI-induced downregulation of VEGF was attributed to inhibition of NFκB, but the role of NFκB in regulating VEGF has become controversial. For example, expression of a mutant IκBα construct did not inhibit VEGF expression in human head and neck squamous cell carcinomas but strongly inhibited the expression of VEGF in human PC3 prostate cancer cells (12,13,43). Furthermore, the inhibitory effects of proteasome inhibitors on VEGF expression are paradoxical given the well established role VHL- and proteasome- mediated degradation plays in the control of HIF-1 protein expression. Therefore, we set out to identify the mechanisms of proteasome inhibitor-mediated downregulation of VEGF, using human prostate cancer and bladder cancer cells as our models. Our

results demonstrate that PIs downregulate HIF-1 protein and transcriptional activity via a phospho-eIF2 -dependent mechanism. Other studies have shown that bortezomib has inhibitory effects on HIF-1 -dependent transcriptional activity regardless of whether or not the protein accumulates (44,45). Consistent with this conclusion, HIF-1α-dependent transcriptional and VEGF expression were also blocked by proteasome inhibitors in DU145 and 253JB-V cells, even though the PIs promoted HIF-1 accumulation in these two cell lines (Figure 5 and Supplemental Figure 2).

Proteasome inhibitors block protein degradation and promote excessive intracellular protein accumulation, which may lead to ER stress. Recent evidence indicates that some antitumor effects of proteasome inhibitors occur as the result of this ER stress. The initial response to ER stress is termed the UPR, and the early phase of the UPR plays a critical cytoprotective role to limit ER stress (28,46). PERK/eIF2α/ATF4 is one of the three axes of the UPR that integrates the transcriptional and translational responses in stressed cells (23,27,28). Phosphorylated eIF2α sequesters the guanine nucleotide exchange factor eIF2B and inhibits the formation of the ternary translation initiation complex eIF2/GTP/Met-$tRNA_i$, thereby resulting in general translational repression to reduce the nascent protein load within the ER. In addition, eIF2B exists in significantly smaller amounts as compared to eIF2 (about 20~30% of eIF2) (42), and consequently partial phosphorylation of eIF2α is sufficient to inhibit the exchange activity of eIF2B and block translation initiation. Our results implicate the UPR in the mechanisms leading to proteasome inhibitor-mediated downregulation of HIF-1. Downregulation of HIF-1 was closely associated with PERK and eIF2 phosphorylation and translation attenuation. Moreover, knockdown of eIF2 rescued HIF-1 expression, establishing a causal connection between the two events. eIF2 controls the global protein translation initiation and our study also showed that knockdown of eIF2 itself slow down protein translation about 30% (Supplemental Figure 1A). This global effect might alleviate the effects of proteasome inhibitors on protein translation attenuation. In eIF2 -depleted cells, the relative difference of 3H-leucine incorporation between

the untreated and PI-treated samples was reduced as compared to what we observed in cells transfected with the non-specific control siRNA (Supplemental Figure 1B). Our experiments with MEFs further confirmed the causal relationship between eIF2 phosphorylation and HIF-1 downregulation. In eIF2 ^{51AA} mutant MEFs, proteasome inhibitors strongly promoted HIF-1 accumulation as compared to what we observed in the wild type MEFs (Figure 6). It is possible that inhibition of HIF-1 translation plays a direct role in the downregulation of the protein.

The proteasome contains three proteolytic sites in the inner -rings (4). In an attempt to verify the results we obtained with the two chemical inhibitors of the proteasome, we knocked down one (5) or all three (1 , 2 and 5) of the active sites of the proteasome using siRNA and measured the effects on translation and HIF-1 accumulation. We confirmed that knockdown of the active sites inhibited the proteasome's proteolytic activities and induced accumulation of the proteasome substrate, p21 (Supplemental Figure 3). Knockdown of proteasome active site(s) attenuated protein translation, but the effects were much less dramatic than those obtained with the chemical inhibitors. Subunit knockdown caused no obvious HIF-1 downregulation (Supplemental Figure 3). Therefore, we speculate that the quantitative differences between the effects of the PIs and proteasome subunit knockdown on proteasome inhibition and downstream cellular stress probably accounted for the differences observed. A recent study reported that prolonged hypoxia downregulates HIF-1 but the mechanisms are not well characterized (19). Given that hypoxia also induces eIF2 phosphorylation, we suspect that the downregulation of HIF-1 expression observed in cells exposed to prolonged hypoxia also involves the UPR.

Our data confirm that PIs induce PERK phosphorylation in prostate cancer cells (Figure 4), but whether or not PERK activation accounts for the eIF2alpha phosphorylation observed in the cells remains unclear. General control non-derepressible-2 (GCN2) is involved in bortezomib induced eIF2 phosphorylation in MEFs (23,47)., and knockdown of both PERK and GCN2 was required to rescue expression of cyclin D1, which is also downregulated via eIF2 translation

attenuation (31). It will be important to identify the kinase(s) that are responsible for proteasome inhibitor-induced eIF2 phosphorylation in various tumor models because eIF2 initiates the downstream cytoprotective or proapoptotic signals that determine cell fate. Inhibitors of these kinases could modulate the effects of proteasome inhibitors and other agents that affect the UPR. We are currently assessing the roles of PERK and GCN2 in our cells and designing strategies to attempting to isolate high affinity inhibitors of them that could prove to be effective new anti-cancer therapeutic regimens.

We also found that proteasome inhibitors had biphasic effects on HIF-1 protein stability. At early time points proteasome inhibitors induced HIF-1 accumulation, but the effects were transient and HIF-1 was not detectable by 4 h. These observations suggest that proteasome inhibitors do have the expected effects on the VHL-proteasome-mediated destruction of HIF-1 but some other proteolytic system mediates the elimination of the protein at the 4 h time point. Recent studies suggest that autophagy, a lysosome dependent degradation system, is activated during ER stress (48-50), and interestingly, eIF2 phosphorylation appears to activate autophagy in cells exposed to amino acid deprivation or viral infection (29,50). We have shown here that PIs induce eIF2 phosphorylation in the same cells that display HIF-1 downregulation, and our preliminary data also suggest that PIs activate autophagy in these cells (K Zhu manuscript in preparation). Furthermore, chemical inhibitors of autophagy (3-methyladenine or chloroquine) partially rescue HIF-1 protein expression (data not shown), which suggests that autophagy is also involved in the elimination of HIF-1 when the proteasome is blocked. However, the effects of eIF2 regulation were much stronger than those of the autophagy inhibitors, suggesting that eIF2 controls several downstream mechanisms that determine HIF-1 expression, such as translation regulation and non-proteasomal degradation.

In our study, we identified two cell lines that displayed efficient proteasome inhibitor-mediated eIF2 phosphorylation and downregulation of HIF-1 (LNCaP Pro5 and PC3) and two that did not (DU145 and 253 JB-V). Interestingly, the basal levels of eIF2α phosphorylation appeared to

correlate with these differences as DU145 and 253 JB-V cells contained high basal phosphorylated eIF2α and LNCaP Pro5 and PC3 cells did not. However, regardless of these differences, there were no measurable differences in global translation rates among the cell lines as measured by [$_{L\text{-}4,5\text{-}}^{3}$H]Leucine incorporation (Supplemental Figure 4), indicating that basal eIF2 phosphorylation observed in DU145 or 253JB-V did not activate the protein synthesis checkpoint. We do not have an explanation for why eIF2α is phosphorylated at baseline in some tumor cell lines but not others. We suspect that it might be related to the differential response to proteasome inhibition induced UPR in different cancer cells and this difference may have very important implications with regard to the molecular mechanism that mediates proteasome inhibitor sensitivity and resistance. Interestingly, PIs strongly inhibited VEGF expression in the 253 JB-V cells despite causing HIF-1 accumulation (Supplemental Figure 2). Thus, PIs can inhibit VEGF expression in cells that fail to activate the UPR, but the mechanisms involved await further study. A previous study showed that eIF2 phosphorylation can also activate NFκB in MEFs during ER stress via repression of the short-lived inhibitor, IκBα (30). However, this observation does not help to explain the effects of PIs on VEGF expression, because we show here the IKK/NFκB inhibitor PS-1145 did not reduce VEGF expression in cells exposed to hypoxia (Figure 2B).

Given that overexpression of HIF-1 promotes tumor angiogenesis and metastasis and confers chemo- and radio-therapy resistance, many approaches have been taken to identify agents that inhibit HIF-1α activity. Several anti-tumor/anti-angiogenic agents have been reported to interfere HIF-1 signaling cascades directly or indirectly, including 2-methoxyestradiol, cetuximab, and PX-478, among others (14,17,51,52). Our data provide evidence that proteasome inhibitors are also potent HIF-1α antagonists. The recognition that VEGF is the primary stimulus of angiogenesis in tumors has also led to the generation of many strategies to inhibit VEGF signaling pathway, but successful inhibition of the VEGF/VEGF receptor signaling pathway may lead to hypoxia and consequent upregulation of HIF-1 expression, producing

undesirable effects (53). Therefore, combination therapy with VEGF pathway and proteasome inhibitors may lead to more complete inhibition of angiogenesis than is observed with either type of agent alone. Clinical trials employing bortezomib plus VEGF pathway inhibitors are currently open at our institution and others.

REFERENCES

1. Adams, J., and Kauffman, M. (2004) *Cancer Invest* **22**(2), 304-311
2. Adams, J. (2004) *Cancer Cell* **5**(5), 417-421
3. Adams, J. (2002) *Trends Mol Med* **8**(4 Suppl), S49-54
4. Adams, J. (2002) *Curr Opin Oncol* **14**(6), 628-634
5. Chauhan, D., Catley, L., Li, G., Podar, K., Hideshima, T., Velankar, M., Mitsiades, C., Mitsiades, N., Yasui, H., Letai, A., Ovaa, H., Berkers, C., Nicholson, B., Chao, T. H., Neuteboom, S. T., Richardson, P., Palladino, M. A., and Anderson, K. C. (2005) *Cancer Cell* **8**(5), 407-419
6. Ruiz, S., Krupnik, Y., Keating, M., Chandra, J., Palladino, M., and McConkey, D. (2006) *Mol Cancer Ther* **5**(7), 1836-1843
7. Fribley, A. M., Evenchik, B., Zeng, Q., Park, B. K., Guan, J. Y., Zhang, H., Hale, T. J., Soengas, M. S., Kaufman, R. J., and Wang, C. Y. (2006) *J Biol Chem* **281**(42), 31440-31447
8. Zhu, H., Zhang, L., Dong, F., Guo, W., Wu, S., Teraishi, F., Davis, J. J., Chiao, P. J., and Fang, B. (2005) *Oncogene* **24**(31), 4993-4999

9. Hideshima, T., Chauhan, D., Richardson, P., Mitsiades, C., Mitsiades, N., Hayashi, T., Munshi, N., Dang, L., Castro, A., Palombella, V., Adams, J., and Anderson, K. C. (2002) *J Biol Chem* **277**(19), 16639-16647

10. Lashinger, L. M., Zhu, K., Williams, S. A., Shrader, M., Dinney, C. P., and McConkey, D. J. (2005) *Cancer Res* **65**(11), 4902-4908

11. Egger, L., Madden, D. T., Rheme, C., Rao, R. V., and Bredesen, D. E. (2007) *Cell Death Differ*

12. Kamat, A. M., Karashima, T., Davis, D. W., Lashinger, L., Bar-Eli, M., Millikan, R., Shen, Y., Dinney, C. P., and McConkey, D. J. (2004) *Mol Cancer Ther* **3**(3), 279-290

13. Williams, S., Pettaway, C., Song, R., Papandreou, C., Logothetis, C., and McConkey, D. J. (2003) *Mol Cancer Ther* **2**(9), 835-843

14. Semenza, G. L. (2003) *Nat Rev Cancer* **3**(10), 721-732

15. Semenza, G. L. (2004) *Cancer Cell* **5**(5), 405-406

16. Manalo, D. J., Rowan, A., Lavoie, T., Natarajan, L., Kelly, B. D., Ye, S. Q., Garcia, J. G., and Semenza, G. L. (2005) *Blood* **105**(2), 659-669

17. Semenza, G. L. (2006) *Expert Opin Ther Targets* **10**(2), 267-280

18. Powis, G., and Kirkpatrick, L. (2004) *Mol Cancer Ther* **3**(5), 647-654

19. Kong, X., Alvarez-Castelao, B., Lin, Z., Castano, J. G., and Caro, J. (2007) *J Biol Chem* **282**(21), 15498-15505

20. Alqawi, O., Moghaddas, M., and Singh, G. (2006) *Prostate Cancer Prostatic Dis* **9**(2), 126-135

21. Trastour, C., Benizri, E., Ettore, F., Ramaioli, A., Chamorey, E., Pouyssegur, J., and Berra, E. (2007) *Int J Cancer* **120**(7), 1451-1458

22. Nawrocki, S. T., Carew, J. S., Dunner, K., Jr., Boise, L. H., Chiao, P. J., Huang, P., Abbruzzese, J. L., and McConkey, D. J. (2005) *Cancer Res* **65**(24), 11510-11519

23. Jiang, H. Y., and Wek, R. C. (2005) *J Biol Chem* **280**(14), 14189-14202

24. Fribley, A., Zeng, Q., and Wang, C. Y. (2004) *Mol Cell Biol* **24**(22), 9695-9704

25. Obeng, E. A., Carlson, L. M., Gutman, D. M., Harrington, W. J., Jr., Lee, K. P., and Boise, L. H. (2006) *Blood* **107**(12), 4907-4916

26. Fels, D. R., and Koumenis, C. (2006) *Cancer Biol Ther* **5**(7), 723-728

27. Koumenis, C. (2006) *Curr Mol Med* **6**(1), 55-69

28. Szegezdi, E., Logue, S. E., Gorman, A. M., and Samali, A. (2006) *EMBO Rep* **7**(9), 880-885

29. Kouroku, Y., Fujita, E., Tanida, I., Ueno, T., Isoai, A., Kumagai, H., Ogawa, S., Kaufman, R. J., Kominami, E., and Momoi, T. (2007) *Cell Death Differ* **14**(2), 230-239

30. Deng, J., Lu, P. D., Zhang, Y., Scheuner, D., Kaufman, R. J., Sonenberg, N., Harding, H. P., and Ron, D. (2004) *Mol Cell Biol* **24**(23), 10161-10168

31. Hamanaka, R. B., Bennett, B. S., Cullinan, S. B., and Diehl, J. A. (2005) *Mol Biol Cell* **16**(12), 5493-5501

32. Semenza, G. L., Shimoda, L. A., and Prabhakar, N. R. (2006) *Novartis Found Symp* **272**, 2-8; discussion 8-14, 33-16

33. Chen, L., Uchida, K., Endler, A., and Shibasaki, F. (2007) *J Biol Chem* **282**(17), 12707-12716

34. Gray, M. J., Zhang, J., Ellis, L. M., Semenza, G. L., Evans, D. B., Watowich, S. S., and Gallick, G. E. (2005) *Oncogene* **24**(19), 3110-3120

35. Pages, G., and Pouyssegur, J. (2005) *Cardiovasc Res* **65**(3), 564-573

36. Xu, Q., Briggs, J., Park, S., Niu, G., Kortylewski, M., Zhang, S., Gritsko, T., Turkson, J., Kay, H., Semenza, G. L., Cheng, J. Q., Jove, R., and Yu, H. (2005) *Oncogene* **24**(36), 5552-5560

37. Semenza, G. (2002) *Biochem Pharmacol* **64**(5-6), 993-998

38. Khanbolooki, S., Nawrocki, S. T., Arumugam, T., Andtbacka, R., Pino, M. S., Kurzrock, R., Logsdon, C. D., Abbruzzese, J. L., and McConkey, D. J. (2006) *Mol Cancer Ther* **5**(9), 2251-2260

39. Williams, S. A., and McConkey, D. J. (2003) *Cancer Res* **63**(21), 7338-7344

40. Bi, M., Naczki, C., Koritzinsky, M., Fels, D., Blais, J., Hu, N., Harding, H., Novoa, I., Varia, M., Raleigh, J., Scheuner, D., Kaufman, R. J., Bell, J., Ron, D., Wouters, B. G., and Koumenis, C. (2005) *Embo J* **24**(19), 3470-3481

41. Blais, J. D., Filipenko, V., Bi, M., Harding, H. P., Ron, D., Koumenis, C., Wouters, B. G., and Bell, J. C. (2004) *Mol Cell Biol* **24**(17), 7469-7482

42. Koumenis, C., Naczki, C., Koritzinsky, M., Rastani, S., Diehl, A., Sonenberg, N., Koromilas, A., and Wouters, B. G. (2002) *Mol Cell Biol* **22**(21), 7405-7416

43. Huang, S., Pettaway, C. A., Uehara, H., Bucana, C. D., and Fidler, I. J. (2001) *Oncogene* **20**(31), 4188-4197

44. Kaluz, S., Kaluzova, M., and Stanbridge, E. J. (2006) *Mol Cell Biol* **26**(15), 5895-5907

45. Birle, D. C., and Hedley, D. W. (2007) *Cancer Res* **67**(4), 1735-1743

46. Lin, J. H., Li, H., Yasumura, D., Cohen, H. R., Zhang, C., Panning, B., Shokat, K. M., Lavail, M. M., and Walter, P. (2007) *Science* **318**(5852), 944-949

47. Jiang, H. Y., and Wek, R. C. (2005) *Biochem J* **385**(Pt 2), 371-380

48. Ogata, M., Hino, S., Saito, A., Morikawa, K., Kondo, S., Kanemoto, S., Murakami, T., Taniguchi, M., Tanii, I., Yoshinaga, K., Shiosaka, S., Hammarback, J. A., Urano, F., and Imaizumi, K. (2006) *Mol Cell Biol* **26**(24), 9220-9231

49. Boya, P., Gonzalez-Polo, R. A., Casares, N., Perfettini, J. L., Dessen, P., Larochette, N., Metivier, D., Meley, D., Souquere, S., Yoshimori, T., Pierron, G., Codogno, P., and Kroemer, G. (2005) *Mol Cell Biol* **25**(3), 1025-1040

50. Talloczy, Z., Jiang, W., Virgin, H. W. t., Leib, D. A., Scheuner, D., Kaufman, R. J., Eskelinen, E. L., and Levine, B. (2002) *Proc Natl Acad Sci U S A* **99**(1), 190-195

51. Tonra, J. R., and Hicklin, D. J. (2007) *Immunol Invest* 36(1), 3-23

52. Mabjeesh, N. J., Escuin, D., LaVallee, T. M., Pribluda, V. S., Swartz, G. M., Johnson, M. S., Willard, M. T., Zhong, H., Simons, J. W., and Giannakakou, P. (2003) Cancer Cell 3(4), 363-375

53. Franco, M., Man, S., Chen, L., Emmenegger, U., Shaked, Y., Cheung, A. M., Brown, A. S., Hicklin, D. J., Foster, F. S., and Kerbel, R. S. (2006) Cancer Res 66(7), 3639-3648

FIGURE LEGENDS

Figure 1. Effects of bortezomib and NPI-0052 on HIF-1α, HIF-2α and VEGF expression. A. Concentration dependent effects of proteasome inhibitors on HIF-1α and HIF-2α protein levels. LNCaP Pro5 cells were exposed to increasing concentrations of bortezomib (BZ) or NPI-0052 (NPI) for 12 h under normoxic or hypoxic conditions and HIF-1α was measured by immunoblotting. **B.** Effects of proteasome inhibitors on HIF-1α transcriptional activity. LNCaP Pro5 cells were exposed to 100 nM bortezomib or 100 nM NPI-0052 for 8 h under normoxic or hypoxic conditions. HIF–1α transcriptional activities were measured using an HRE-driven *Firefly* luciferase expression construct and a *Renilla* luciferase construct as an internal normalization control. The results are expressed as relative luciferase activities. *Columns*, mean (n=3); *bars*, standard errors (S.E.), *P<0.001, compared to controls. **C.** Effects of proteasome inhibitors on VEGF expression. LNCaP Pro5 cells were exposed to 100 nM bortezomib or 100 nM NPI-0052 for 12 h or 24 h under normoxic or hypoxic conditions. VEGF expression was measured by VEGF ELISA (R&D System) in conditioned media. *Columns*, mean (n=3); *bars*, S.E., *P<0.001, compared to each control (Ctrl). **D.** Effects of HIF-1α knockdown on VEGF expression. siRNA mediated knockdown of HIF-1α was carried out as described in Materials and Methods. LNCaP Pro5 cells were exposed to 100 nM bortezomib or 100 nM NPI-0052 for 24 h and VEGF expression was measured by VEGF ELISA (R&D System). *Columns*, mean (n=3); *bars*, S.E., *P<0.001, compared to control. In parallel, HIF-1α expression was examined to confirm the silencing efficiency and actin served as a loading control (right).

Figure 2. Effects of proteasome inhibitors on other candidate VEGF promoter regulators. A. Effects of proteasome inhibitors on other VEGF promoter regulators. LNCaP Pro5 cells were exposed to 100 nM bortezomib (BZ) or 100 nM NPI-0052 (NPI) for 12 h under hypoxic conditions. Total lysates were probed for expression of HIF-1α, HIF-1β, STAT3, p300 or Ref-1 by immunoblotting and actin levels were measured as a loading control. Similar results were obtained in 3 independent experiments. **B.**

Effects of PS-1145 on VEGF expression. LNCaP Pro5 cells were exposed to 10 μM or 20 μM PS-1145, 100 nM bortezomib (BZ), or 100 nM NPI-0052(NPI) for 24 h under normoxic or hypoxic conditions. VEGF levels were measured by ELISA (R&D System) in conditioned media. *Columns*, mean (n=3); *bars*, S.E., *P<0.001, compared to each control.

Figure 3. Effects of proteasome inhibitors on HIF-1α mRNA levels and protein stability. A. Effects of proteasome inhibitors on HIF-1α mRNA levels. LNCaP Pro5 cells were exposed to 100 nM bortezomib (BZ) or 100 nM NPI-0052 (NPI) for 12 h under normoxic or hypoxic conditions. Total cellular mRNA was extracted and reverse transcribed into first strand cDNAs. Real time PCR for HIF-1α was performed using the BioRad iCycler. The expression of HIF-1α was normalized against GAPDH level and the ratio in the untreated group was arbitrarily set at the value of 1. *Columns*, mean (n=3); *bars*, S.E. **B.** Biphasic effects of proteasome inhibitors on HIF-1α stability. LNCaP Pro5 cells were preincubated with 50 μM $CoCl_2$ for 16 h, then exposed to 100 nM bortezomib (BZ) or 100 nM NPI-0052 (NPI) with or without 20 μM cycloheximde (CHX) for the time indicated in the presence of $CoCl_2$. Total lysates were probed for HIF-1α expression by immunoblotting and actin levels served as a loading control. Similar results were obtained from 3 independent experiments. **C.** Densitometric quantification and statistical analysis of three independent repetitions of the experiment described above. HIF-1α /actin levels from untreated cells were arbitrarily set at the value of 1. HIF-1α signals following normalization to actin levels were expressed as relative densitometry units of the mean of the three repetitions. *Columns*, mean (n=3); *bars*, S.E., *P<0.01, compared to control group.

Figure 4. Effects of proteasome inhibitors on the unfolded protein response. A. Proteasome inhibitors induce PERK phosphorylation. LNCaP Pro5 cells were exposed to 100 nM bortezomib (BZ), 100 nM NPI-0052 (NPI) or 10 M thapsigargin (TG) for 4 h under normoxic conditions, and phosphorylated PERK and actin levels were measured by immunoblotting. Similar results were obtained in 3 independent

experiments. **B.** Proteasome inhibitors induce eIF2 phosphorylation. LNCaP Pro5 cells were exposed to 100 nM bortezomib (BZ), 100 nM NPI-0052 (NPI) or 10M thapsigargin (TG) for 4 h under normoxic conditions, and phosphorylated eIF2 and total eIF2α levels were measured by immunoblotting. The numbers located below each lane correspond to the quantification of the phosphorylated eIF2α signals by densitometry adjusted to the total eIF2α protein levels. The phosphorylation of eIF2α in the untreated group is arbitrarily set at the value of 1. Similar results were obtained in 3 independent experiments. **C.** Proteasome inhibitors attenuate protein synthesis. LNCaP Pro5 cells were exposed to 100 nM bortezomib, 100 nM NPI-0052, 10 μM thapsigargin (TG) or 40 μM cycloheximide (CHX) for 4 h under normoxic conditions and protein synthesis was measured by [$_{L\text{-}4,5\text{-}}{}^{3}$H]Leucine incorporation. The incorporation of [$_{L\text{-}4,5\text{-}}{}^{3}$H]Leucine in the untreated group was arbitrarily set at the value of 1. *Columns*, mean (n=3); *bars*, S.E., *P<0.001. **D.** Effects of thapsigargin (TG) or tunicamycin (TM) on HIF-1α protein levels. LNCaP Pro5 cells were incubated with 100 nM bortezomib (BZ), 100 nM NPI-0052 (NPI), 10 μM thapsigargin (TG) or 5 μg/ml tunicamycin (TM) for 12 h under hypoxic conditions and HIF-1α levels in total lysates were determined by immunoblotting. Actin levels served as loading controls. Similar results were obtained in 3 independent experiments.

Figure 5. Differential effects of proteasome inhibitors on UPR and HIF-1α protein levels in different cancer cells. A. Differential effects of proteasome inhibitors on eIF2α phosphorylation. PC3, DU145 and 253JB-V cells were incubated with 100 nM bortezomib (BZ), 100 nM NPI-0052 (NPI), or 10 μM thapsigargin (TG) for 4 h. Phosphorylated eIF2α at Ser52 and total eIF2α levels in total lysates were measured by immunoblotting. The numbers located below each lane corresponded to the levels of eIF2α phosphorylation which were determined by densitometry analysis and adjusted to total eIF2α protein levels. The phosphorylation of eIF2α in the untreated group was arbitrarily set at the value of 1. Similar results were obtained in 3 independent experiments. **B.** Differential effects of proteasome inhibitors on protein synthesis. PC3, DU145 and 253JB-V cells were exposed to 100 nM bortezomib

(BZ), 100 nM NPI-0052 (NPI) or 10 μM thapsigargin (TG) for 4 h and protein synthesis was measured by [$_{L\text{-}4,5\text{-}}^{3}$H]Leucine incorporation. The incorporation of [$_{L\text{-}4,5\text{-}}^{3}$H]Leucine in the untreated group was arbitrarily set at 1. *Columns*, mean (n=3); *bars*, S.E., *P<0.001, compared to control. **C.** Differential effects of proteasome inhibitors on HIF-1α. PC3, DU145 and 253JB-V cells were incubated with 100 nM bortezomib (BZ) or 100 nM NPI-0052 (NPI) for 12 h under hypoxic conditions and HIF-1 levels were measured in total lysates by immunoblotting. Actin levels were measured as loading controls. Similar results were obtained in 3 independent experiments.

Figure 6. Effects of eIF2α regulation on HIF-1α expression and protein synthesis. A. LNCaP Pro5 cells were transfected with a siRNA construct specific for eIF2 or a non-targeted control siRNA as described in Materials and Methods. Transfected cells were incubated with 100 nM bortezomib (BZ), 10 nM NPI-0052 (NPI) or 5 μM thapsigargin (TG) for 8 h under hypoxic conditions and HIF-1 levels were examined by immunoblotting. Levels of eIF2α were also determined to confirm the silencing efficiency and actin served as a loading control. Similar results were obtained in 3 independent experiments. **B.** Effects of proteasome inhibitors on eIF2 and protein translation in MEFs. *Upper panel*. eIF2 ^{51SS}-MEFs and eIF2 ^{51AA}-MEFs were exposed to 100nM bortezomib (BZ), 100nM NPI-0052 (NPI) or 5μM thapsigargin (TG) for 4 h and phosphorylated and total eIF2α levels were measured by immunoblotting. *Lower panel*. Protein synthesis was measured by [$_{L\text{-}4,5\text{-}}^{3}$H]Leucine incorporation. The incorporation of [$_{L\text{-}4,5\text{-}}^{3}$H]Leucine in the untreated group was arbitrarily set at the value of 1. *Columns*, mean (n=2); *bars*, S.E. **C.** Effects of proteasome inhibitors on HIF-1 in MEFs. eIF2 ^{51SS}-MEFs and eIF2 ^{51AA}-MEFs were exposed to 100 nM bortezomib (BZ), 100 nM NPI-0052 (NPI) or 5μM thapsigargin (TG) for 12 h under hypoxic conditions. HIF-1α levels were measured by immunoblotting and total eIF2 and actin served as loading controls.

SUPPLEMENTAL FIGURE LEGENDS

Sup Figure 1. Effects of knocking down eIF2 on protein translation in LNCaP Pro5 cells. A. LNCaP Pro5 cells were transfected with a siRNA construct specific for eIF2α or a non-targeted control siRNA as described in Materials and Methods. Protein synthesis was measured by [$_{L\text{-}4,5\text{-}}^{3}$H]Leucine incorporation and the incorporation of [$_{L\text{-}4,5\text{-}}^{3}$H]Leucine in the non-targeted control group was arbitrarily set at 1. *Columns*, mean (n=3); *bars*, S.E. **B.** Transfected cells were incubated with 100 nM bortezomib (BZ), 100 nM NPI-0052 (NPI) or 5 μM thapsigargin (TG) for 8 h and protein synthesis was measured by [$_{L\text{-}4,5\text{-}}^{3}$H]Leucine incorporation. The incorporation of [$_{L\text{-}4,5\text{-}}^{3}$H]Leucine in the untreated group was arbitrarily set at 1. *Columns*, mean (n=3); *bars*, S.E. **C.** Levels of eIF2α were determined to confirm the silencing efficiency and actin served as a loading control.

Sup Figure 2. Effects of proteasome inhibitors on VEGF expression in 253 JB-V and DU145 cells. 253JB-V and DU145 cells were exposed 100 nM bortezomib (BZ) or 100 nM NPI-0052 (NPI) for 24 h under normoxic conditions. VEGF levels were measured by ELISA (R&D System) in the conditioned media. *Columns*, mean (n=3); *bars*, S.E., *P<0.05.

Sup Figure 3. Effects of knocking down proteasome active subunit(s) on HIF-1 protein expression and protein translation in LNCaP Pro5 cells. A. LNCaP Pro5 cells were transfected with a siRNA construct specific for proteasome subunit 5 or a non-targeted control siRNA for 36 h. LNCaP Pro5 cells transfected with non-targeted control siRNA were incubated with 100nM bortezomib (BZ), 100nM NPI-0052 (NPI) under hypoxic conditions for 12 h. LNCaP Pro5 cells depleted of 1 were incubated for 12 h under hypoxic conditions without treatment. Levels of HIF-1, p21 and proteasome subunit 5 were examined by immunoblotting and actin served as a loading control. Similar results were obtained in 3 independent experiments. **B.** The same experiments were performed in LNCaP Pro5 cells as in Sup Fig. 3A and protein synthesis was measured by [$_{L\text{-}4,5\text{-}}^{3}$H]Leucine incorporation. The incorporation of [$_{L\text{-}4,5\text{-}}^{3}$H]Leucine in the untreated group was arbitrarily set at 1. *Columns*, mean (n=3); *bars*, S.E. **C.** The trypsin-like activity of 20S proteasome measured with Boc-LRR-amc was determined by measurement of

fluorescence generated from the cleavage of the fluorigenic substrate. Release of fluorescence (amc) was measured using a spectrofluorometer using an excitation of 380 nm and an emission of 460 nm. Proteasome activity was evaluated in relative fluorescence units (RFU) and the RFU in the non-targeted control group was arbitrarily set at 100. *Columns*, mean (n=3); *bars*, S.E. **D.** LNCaP Pro5 cells were transfected with siRNA constructs specific for proteasome subunits 1 , 2 and 5 or a non-targeted control siRNA for 36 h. Cells transfected with non-targeted control siRNA were incubated with 100 nM bortezomib (BZ), 100 nM NPI-0052 (NPI) for 12 h under hypoxic conditions and cells depleted 1 , 2 and 5 were incubated for 12 h under hypoxic conditions without treatment. Levels of HIF-1, proteasome subunit 1 , 2 and 5 were examined by immunoblotting and actin served as a loading control. Similar results were obtained in 3 independent experiments. **E.** The same experiments were performed in LNCaP Pro5 cells as in Sup Fig. 3D and protein synthesis was measured by [$_{L\text{-}4,5\text{-}}$^{3}H]Leucine incorporation. The incorporation of [$_{L\text{-}4,5\text{-}}$^{3}H]Leucine in the untreated group was arbitrarily set at 1. *Columns*, mean (n=3); *bars*, S.E. **F.** The trypsin-like activity of 20S proteasome of LNCaP Pro5 cells measured with Boc-LRR-amc was determined by measurement of fluorescence generated from the cleavage of the fluorigenic substrate. Release of fluorescence (amc) was measured using a spectrofluorometer using an excitation of 380nm and an emission of 460nm. Proteasome activity was evaluated in RFU and the RFU in the non-targeted control group was arbitrarily set at 100. *Columns*, mean (n=3); *bars*, S.E.

Sup Figure 4. Comparison of basal protein synthesis in four genitourinary cancer cell lines. LNCaP Pro5, PC3, DU145 and 253JB-V cells were plated in 6-well plates at 1x10^{6} cells /well and attached for 24 h. Protein synthesis was measured by [$_{L\text{-}4,5\text{-}}$^{3}H]Leucine incorporation. The incorporation in [$_{L\text{-}4,5\text{-}}$^{3}H]Leucine of LNCaP Pro5 cells was arbitrarily set at 1. *Columns*, mean (n=2); *bars*, S.E.

Figure 1.

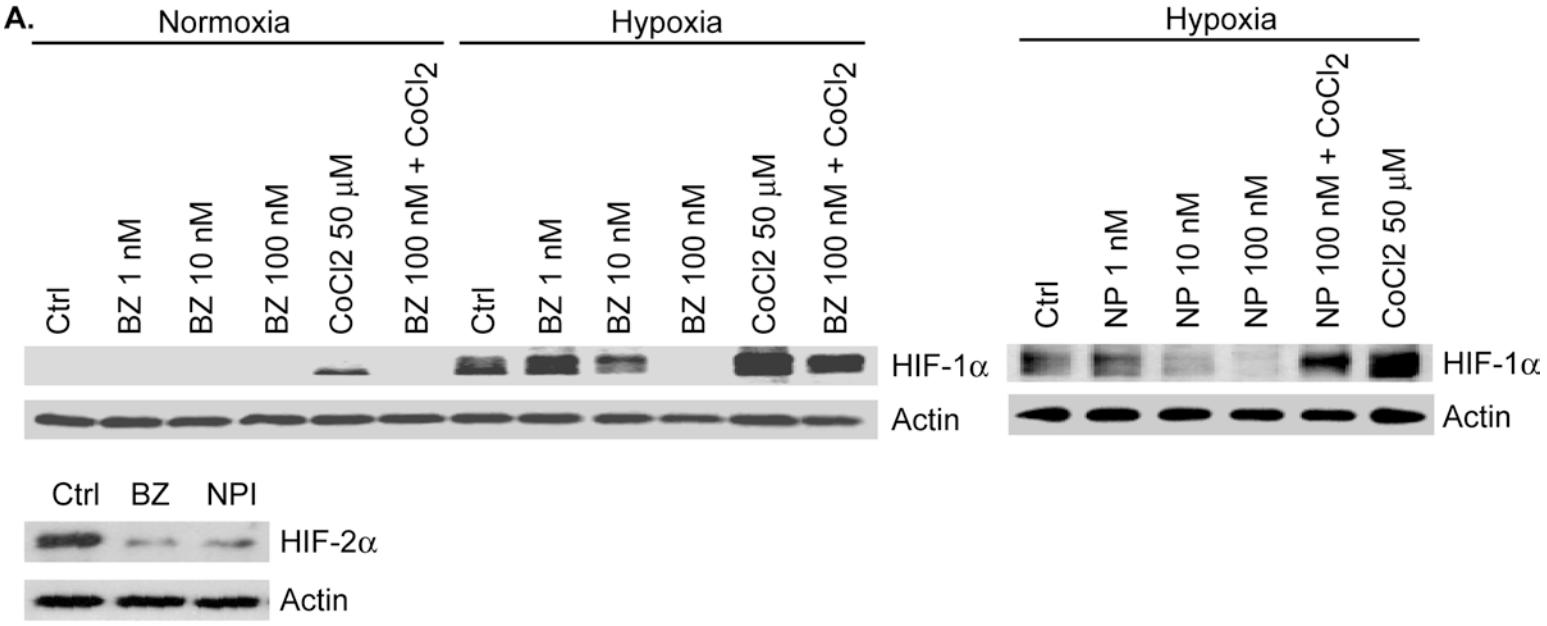
A.
Normoxia
Hypoxia
Hypoxia
Ctrl
BZ 1 nM
BZ 10 nM
BZ 100 nM
CoCl2 50 μM
BZ 100 nM + CoCl2
Ctrl
BZ 1 nM
BZ 10 nM
BZ 100 nM
CoCl2 50 μM
BZ 100 nM + CoCl2
Ctrl
NP 1 nM
NP 10 nM
NP 100 nM
NP 100 nM + CoCl2
CoCl2 50 μM
HIF-1α
Actin
HIF-1α
Actin
Ctrl BZ NPI
HIF-2α
Actin

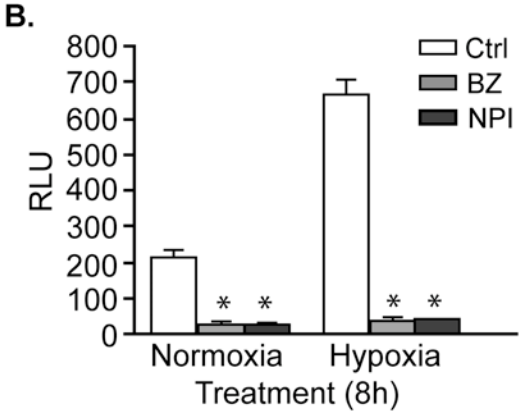
B.
RLU
Ctrl
BZ
NPI
Normoxia
Hypoxia
Treatment (8h)

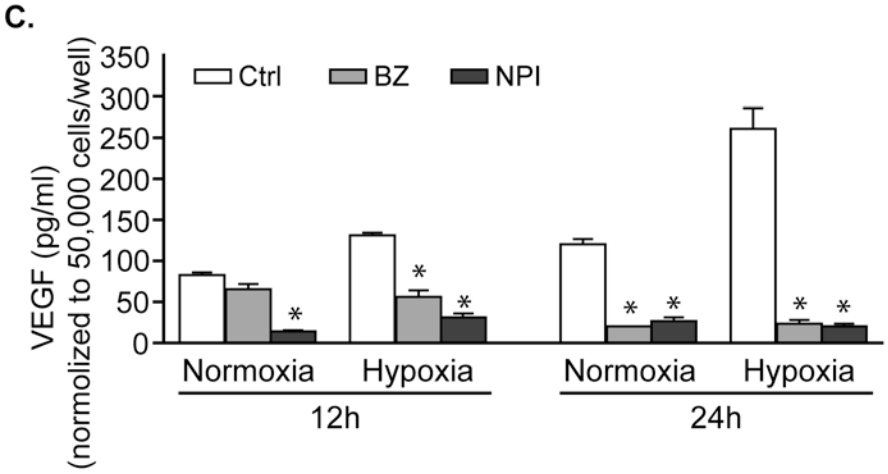
C.
VEGF (pg/ml)
(normolized to 50,000 cells/well)
Ctrl
BZ
NPI
Normoxia
Hypoxia
12h
Normoxia
Hypoxia
24h

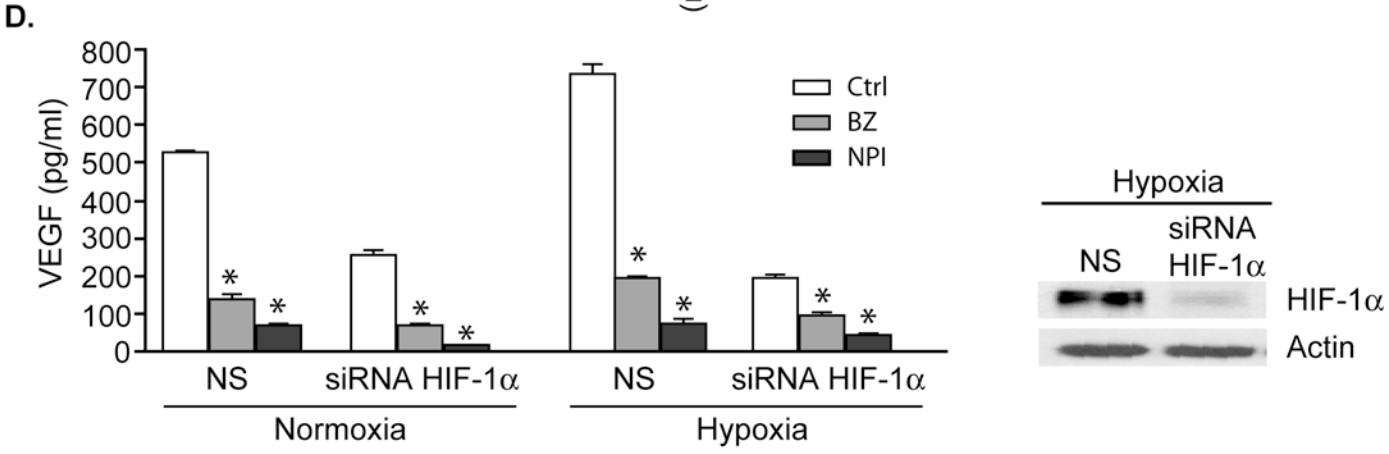
D.
VEGF (pg/ml)
Ctrl
BZ
NPI
NS
siRNA HIF-1α
NS
siRNA HIF-1α
Normoxia
Hypoxia
Hypoxia
NS
siRNA HIF-1α
HIF-1α
Actin

Supplement Figure 1

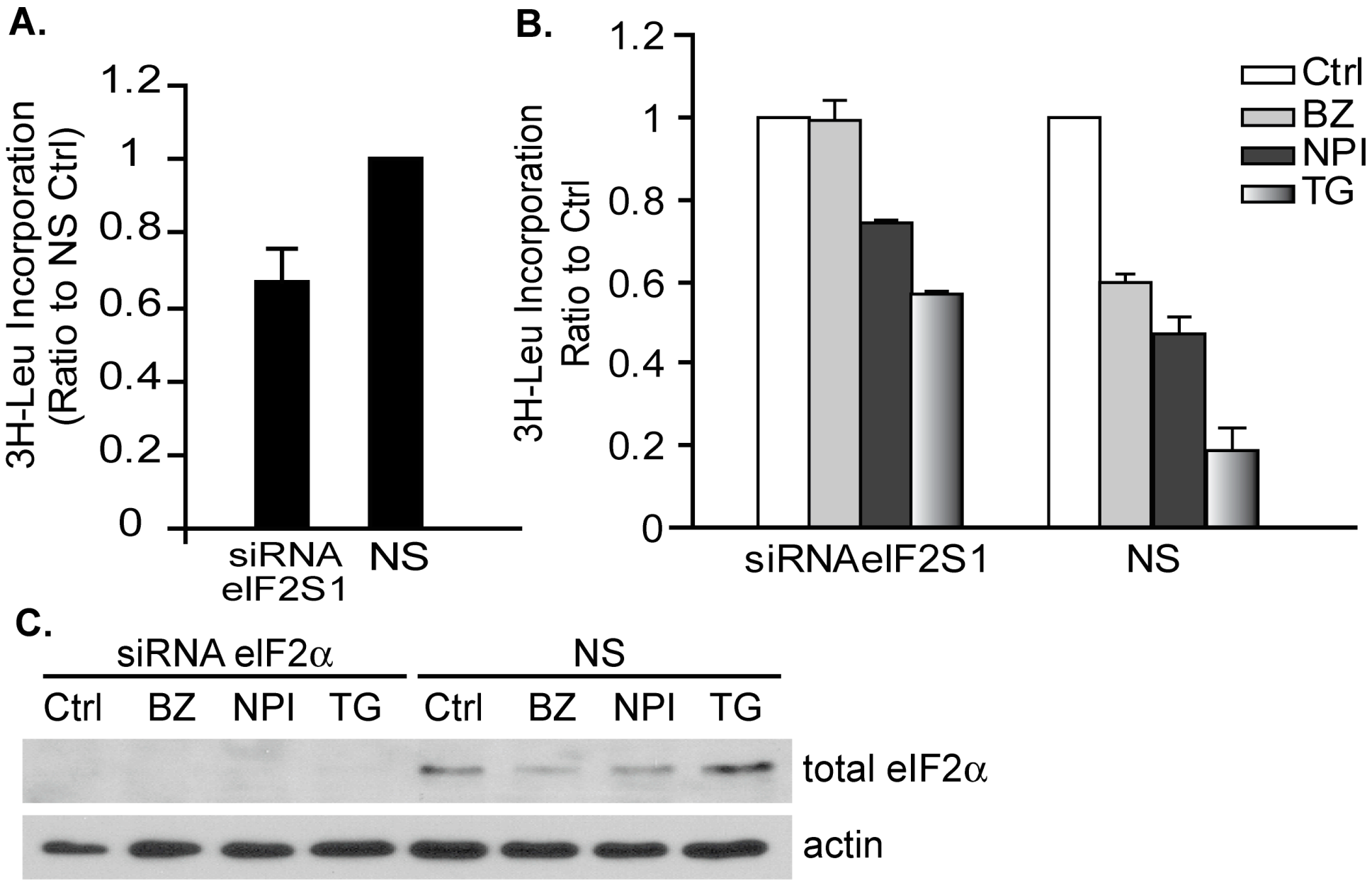

Figure 2

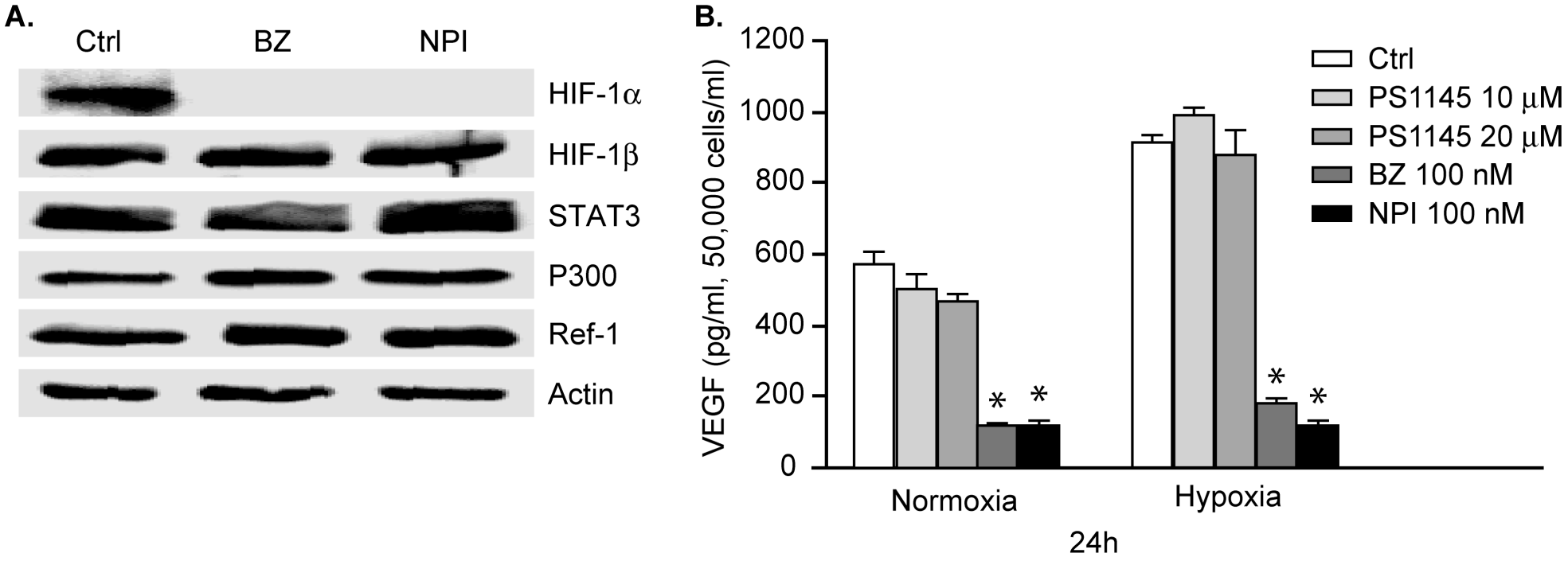
A.
Ctrl
BZ
NPI
HIF-1α
HIF-1β
STAT3
P300
Ref-1
Actin
B.
VEGF (pg/ml, 50,000 cells/ml)
1200
1000
800
600
400
200
0
Ctrl
PS1145 10 μM
PS1145 20 μM
BZ 100 nM
NPI 100 nM
*
*
*
*
Normoxia
Hypoxia
24h

Figure 3

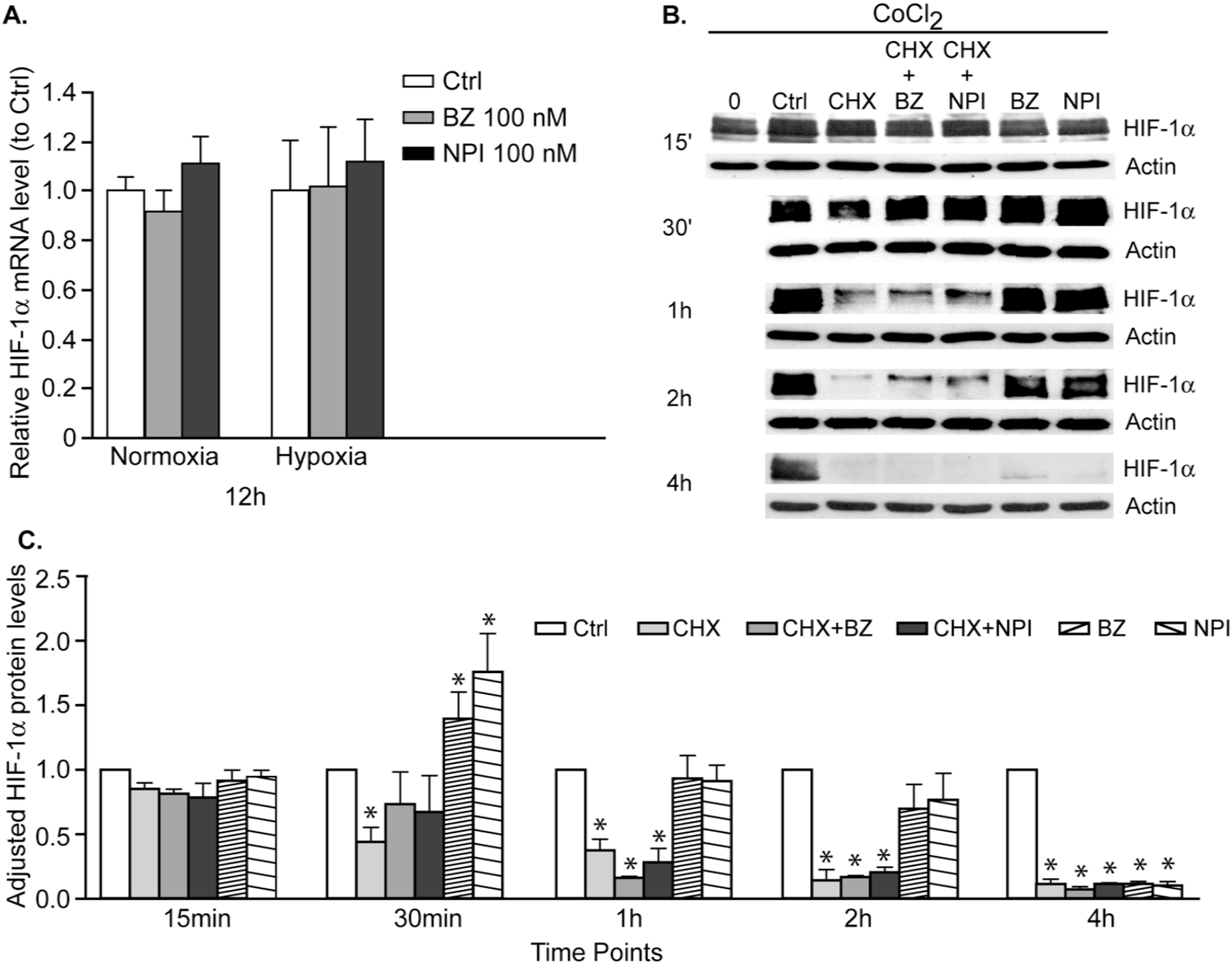
A.
Relative HIF-1α mRNA level (to Ctrl)
1.4
1.2
1.0
0.8
0.6
0.4
0.2
0
Ctrl
BZ 100 nM
NPI 100 nM
Normoxia
Hypoxia
12h
B.
CoCl2
CHX + BZ
CHX + NPI
0
Ctrl
CHX
BZ
NPI
BZ
NPI
15'
30'
1h
2h
4h
HIF-1α
Actin
C.
Adjusted HIF-1α protein levels
2.5
2.0
1.5
1.0
0.5
0.0
Ctrl
CHX
CHX+BZ
CHX+NPI
BZ
NPI
15min
30min
1h
2h
4h
Time Points

Figure 4

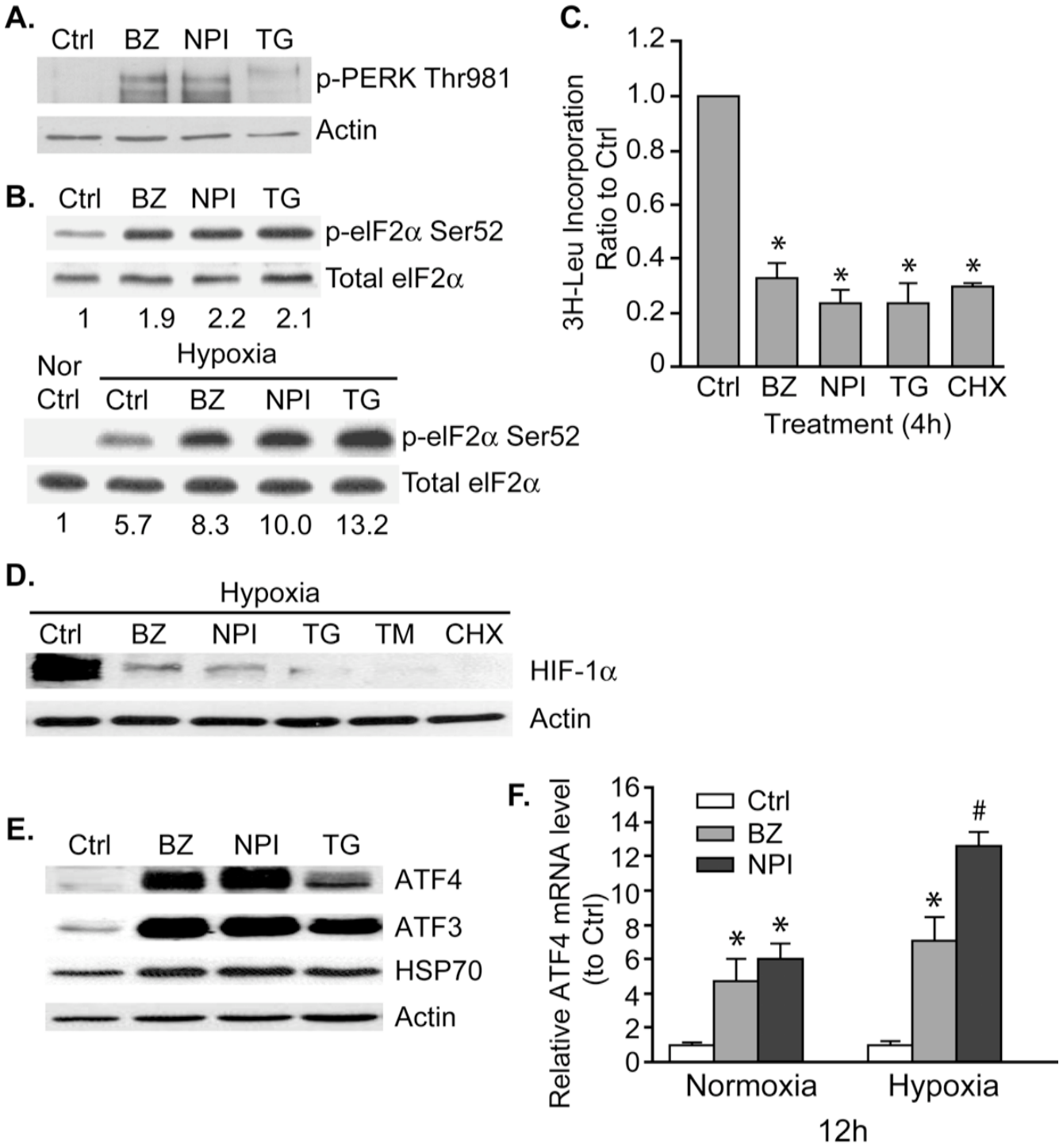
A.
Ctrl
BZ
NPI
TG
p-PERK Thr981
Actin
B.
Ctrl
BZ
NPI
TG
p-eIF2α Ser52
Total eIF2α
1
1.9
2.2
2.1
Nor Ctrl
Hypoxia
Ctrl
BZ
NPI
TG
p-eIF2α Ser52
Total eIF2α
1
5.7
8.3
10.0
13.2
C.
3H-Leu Incorporation Ratio to Ctrl
1.2
1.0
0.8
0.6
0.4
0.2
0
Ctrl
BZ
NPI
TG
CHX
Treatment (4h)
D.
Hypoxia
Ctrl
BZ
NPI
TG
TM
CHX
HIF-1α
Actin
E.
Ctrl
BZ
NPI
TG
ATF4
ATF3
HSP70
Actin
F.
Relative ATF4 mRNA level (to Ctrl)
16
14
12
10
8
6
4
2
0
Ctrl
BZ
NPI
Normoxia
Hypoxia
12h

Figure 5

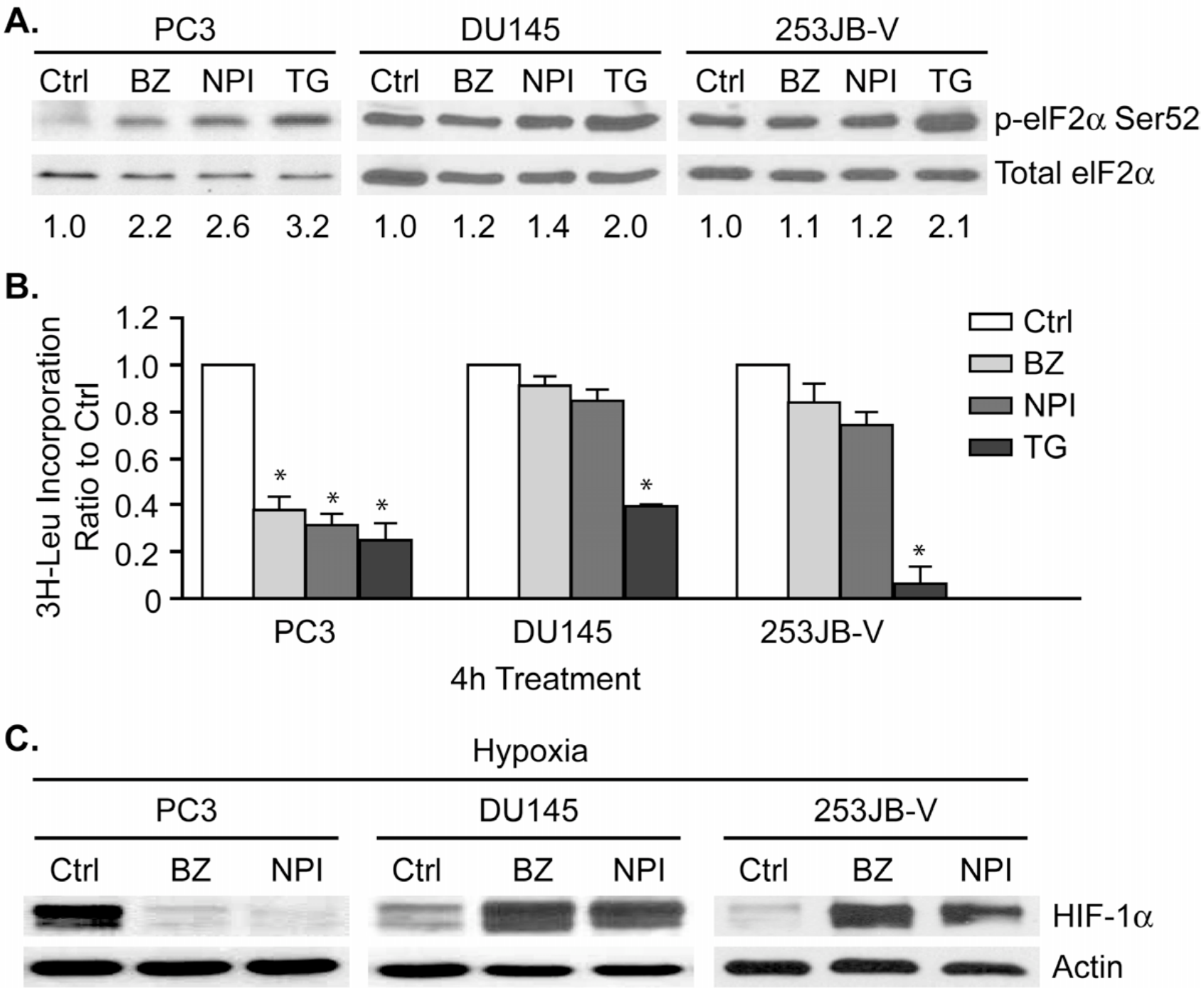
A.
PC3
DU145
253JB-V
Ctrl
BZ
NPI
TG
p-eIF2α Ser52
Total eIF2α
1.0 2.2 2.6 3.2
1.0 1.2 1.4 2.0
1.0 1.1 1.2 2.1
B.
3H-Leu Incorporation Ratio to Ctrl
1.2
1.0
0.8
0.6
0.4
0.2
0
Ctrl
BZ
NPI
TG
PC3
DU145
253JB-V
4h Treatment
C.
Hypoxia
PC3
DU145
253JB-V
Ctrl
BZ
NPI
HIF-1α
Actin

Figure 6

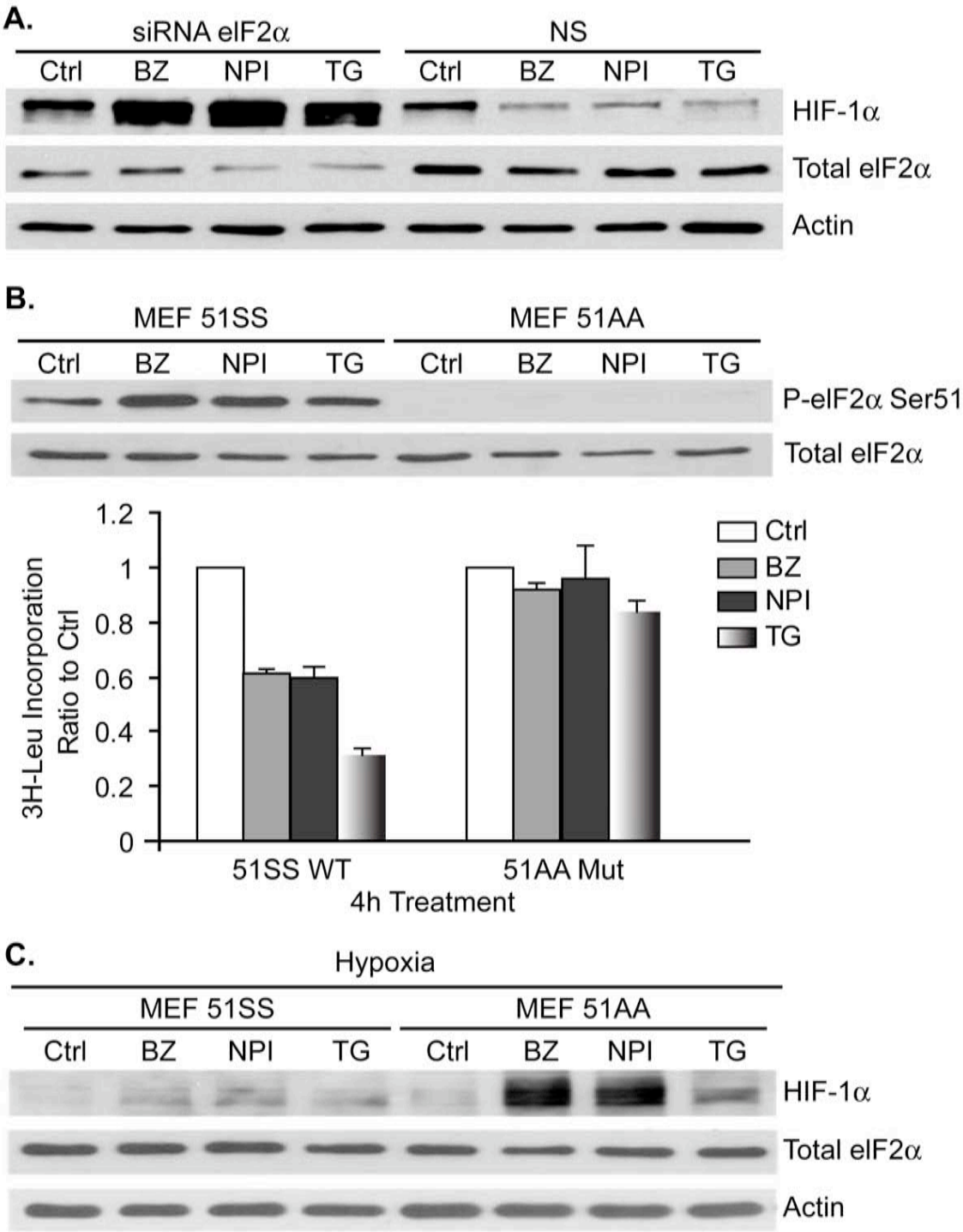
A.
siRNA eIF2α
NS
Ctrl
BZ
NPI
TG
Ctrl
BZ
NPI
TG
HIF-1α
Total eIF2α
Actin
B.
MEF 51SS
MEF 51AA
Ctrl
BZ
NPI
TG
Ctrl
BZ
NPI
TG
P-eIF2α Ser51
Total eIF2α
3H-Leu Incorporation
Ratio to Ctrl
1.2
1
0.8
0.6
0.4
0.2
0
Ctrl
BZ
NPI
TG
51SS WT
51AA Mut
4h Treatment
C.
Hypoxia
MEF 51SS
MEF 51AA
Ctrl
BZ
NPI
TG
Ctrl
BZ
NPI
TG
HIF-1α
Total eIF2α
Actin

Supplement Figure 2

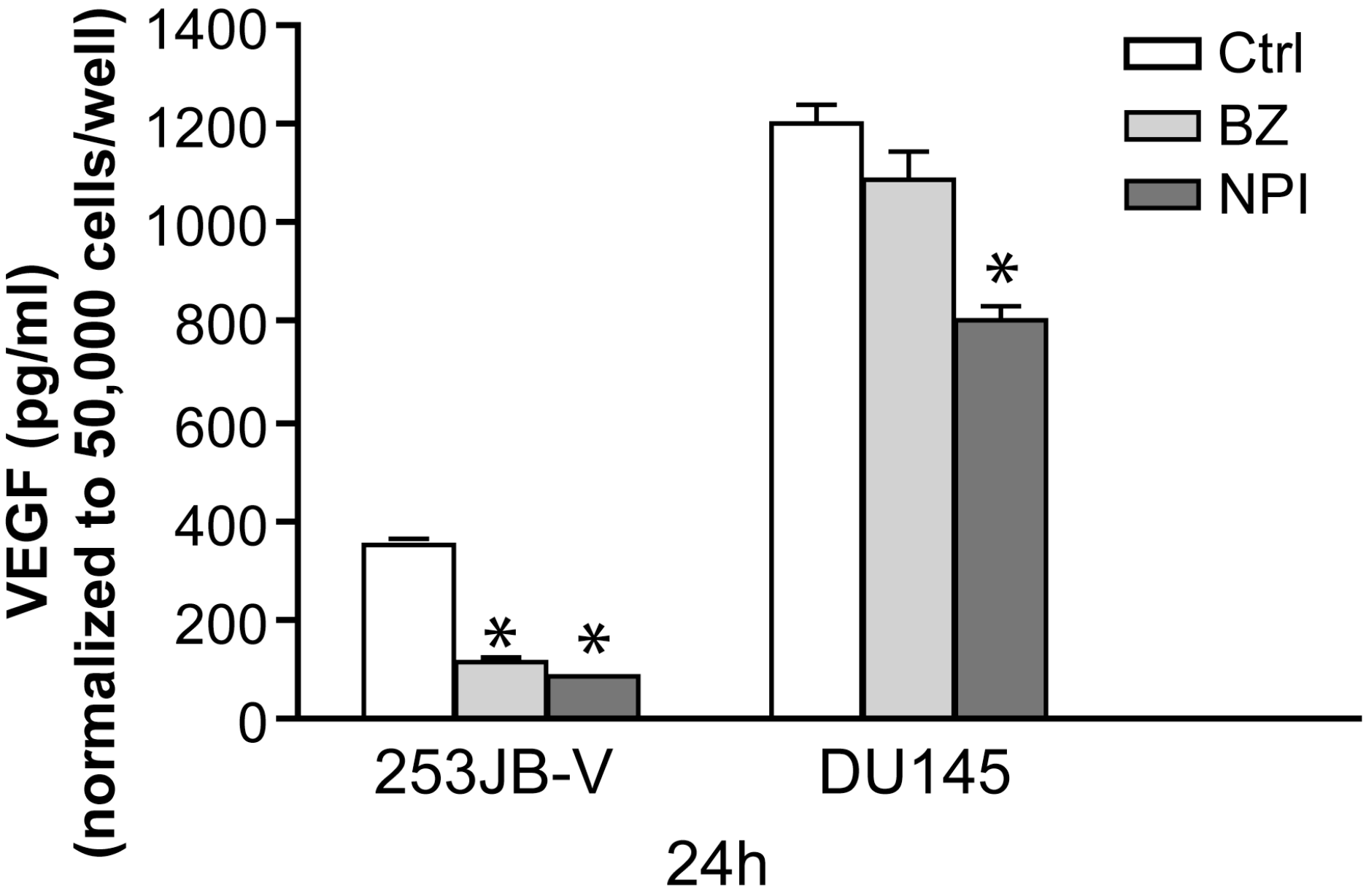

Supplement Figure 4

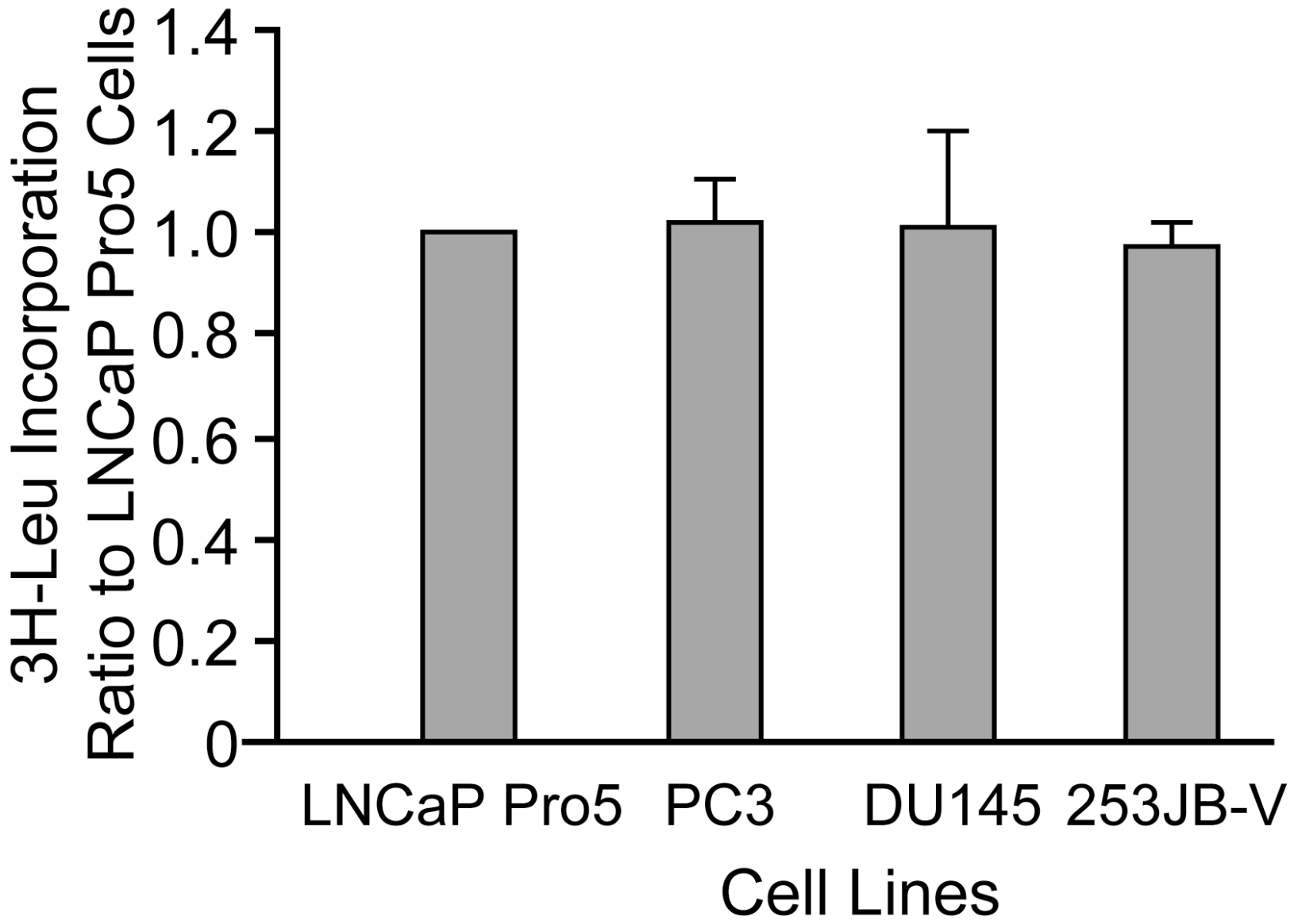

Supplement Figure 3